Paleofloral dependence of coal methane sorption capacity

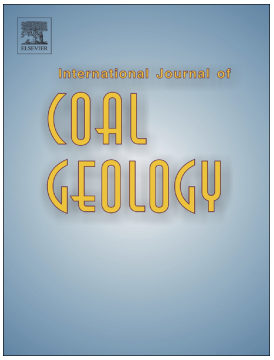

Paleofloral dependence of coal methane sorption capacity

Andreas Busch, Fengshuang Han, Clayton R. Magill

PII: S0166-5162(19)30383-0
DOI: https://doi.org/10.1016/j.coal.2019.103232
Article Number: 103232
Reference: COGEL 103232

To appear in: *International Journal of Coal Geology*

Received date: 7 April 2019
Revised date: 25 June 2019
Accepted date: 26 June 2019

Please cite this article as: A. Busch, F. Han and C.R. Magill, Paleofloral dependence of coal methane sorption capacity, International Journal of Coal Geology, https://doi.org/10.1016/j.coal.2019.103232

Paleofloral Dependence of Coal Methane Sorption Capacity

Andreas Busch[1*], *Fengshuang Han*[1,2], *Clayton R. Magill*[1]

[1]The Lyell Centre, Heriot-Watt University, Edinburgh, Scotland, UK

[2]Ningbo University of Technology, School of Materials and Chemical Engineering/School of Safety Engineering, China

Abstract

The aim of this study is to reveal key physiochemical factors controlling gas sorption in coals since and during periods of dramatic coal deposition in Earth's history – the Upper Carboniferous (326–299 Ma) and Permian (299–252 Ma). As a starting point we developed a database of about 1000 entries, including coal-specific parameters such as proximate and ultimate analysis, sample origin, and specific surface area. Our study proposes an innovative approach that links emerging, quantitative organic molecular analyses with more established bulk (bio)geochemical techniques as a context for (1) describing gas–coal (i.e., coalbed methane) formations, (2) sweet-spot identification in terms of methane sorption potential. We found that the main controlling parameter is coal age; Permian coals adsorb significantly more methane than Carboniferous coals at comparable maturity. This difference is reflected in micropore surface area and oxygen content of the two sets, with Permian having higher values than the corresponding Carboniferous coals. We attribute this difference in Langmuir volume or surface area to the original plant material, expressed through differences in the molecular structures and surface chemistries of the sorption sites which is also clearly reflected in a lower aromaticity for Permian coals. This leads to a more detailed view on the evolution of original plant material from the Carboniferous to Permian age, coinciding with an evolution in plant material, specifically lignite, changes in climatic conditions towards more arid environments, possible changes in water compositions and bacterial activities.

* a.busch@hw.ac.uk

1 Introduction

Different relationships have been published to relate methane sorption capacity to various coal properties, such as maceral composition or coal maturity. However, so far no clear picture has been drawn to provide a universally applicable description that can be applied across different coal basins of different age or rank. Parameters that have a negative effect on the sorption capacity are water and ash yield (or mineral matter content) content (Busch and Gensterblum, 2011). While it seems sensible to assume that ash yield has a negative impact on sorption capacity, clear evidence is not provided, especially when considering that clay minerals can form a substantial share of the sorption capacity and clays are known for large specific surface areas, hence significant sorption capacity.

Looking at the evolution of coal with maturity, we can identify some peculiarities that will have direct and indirect impacts on the sorption capacity. Prinz et al. (2004) and Prinz and Littke (2005) studied the structure and sorption capacity of 10 Carboniferous coals from the Ruhr Basin, Germany, ranging in vitrinite reflectance (VRr) from 0.76 to 2.23%. Clear relationships between the micropore (pore size < 2 nm) and the meso/macropore (pore size > 2 nm) systems and rank were identified: For dry coals, the micropore volume decreases with an increase in maturity to about VRr~1.2-1.3%, after which it increases linearly with coal rank. This is different for moist coals where the micropore volume increases linearly with coal rank across the entire maturity range of these coal samples. It should be noted here that the micropore volume of dry and moisture-equilibrated samples at VRr>1.2-1.3% is very similar. Likewise it was found that the equilibrium moisture content decreases to about VRr~1.2-1.3% which is followed again by an increase towards higher rank. This behaviour is reflected in the methane sorption capacity, having a minimum at the minimum of the micropore volume or the equilibrium moisture content (see also Busch and Gensterblum (2011)). In simple terms, coal has relative large average pore sizes at low-rank (hence coals are rather mesoporous) that are filled with water. With an increase in rank, the water is lost due to a decrease in meso/macropore volume and the subsequent formation of micropores. This is coinciding with a decrease in oxygen functional groups. Water is not accessible to a broad fraction of these micropores due to clustering at the pore throats (Prinz and Littke, 2005). At the same time, gases like N_2, CO_2, CH_4 and higher aromatic hydrocarbon gases as well as liquid hydrocarbons form with an increase in maturity (Rice, 1993). These liquid hydrocarbons fill micropores and smaller mesopores, reducing the water holding but also the methane sorption capacity. At the same time coal generally transforms to higher aromaticities. At the onset of hydrocarbon cracking at around VRr~1.2-1.3%, the micropore volume filled by oil droplets successively becomes accessible to gas and water and the decrease in sorption capacity changes to an increase with maturity. This interplay seems valid due to the nature of coal and its transformation with coalification and is schematically illustrated in Figure 1.

A number of studies have been published from either a specific coal field/basin or combining samples from several coal mining areas. One of the first study analysing larger datasets of Permian coals from the Australian Bowen Basin was published by Levy et al. (1997). Authors indicated for dry coals ranging in

fixed carbon content from 60 to about 90%, corresponding to lignite to (semi)-anthracite rank (van Krevelen, 1993), and that higher methane sorption capacities than for their corresponding moist samples were found. Methane sorption capacity was taken at 5 MPa and 30°C. Towards high-rank, an increase in sorption capacity for dry and moist coals was observed. This increase is related to an increase in specific surface area as determined from low pressure CO_2 sorption. In CO_2 low pressure sorption, as opposed to N_2 low pressure sorption, the micropore and lower mesopore range is probed. Most sorption pores are located in this pore size range.

In comparison, the relationship between sorption capacity and maceral composition is ambiguous. Crosdale et al. (1998) found slightly higher capacities for bright (vitrinite rich) compared to dull (inertinite rich) Permian coals from the Bowen Basin. This was supported by Laxminarayana and Crosdale (2002) for Permian Indian coals, and Cretaceous coals from the Gates Formation in Canada (Lamberson and Bustin, 1993). Ettinger et al. (1966b), on the other hand, identified inertinite as a control on the methane sorption capacity, tested on coals from the Russian Carboniferous Petchora and Permian Kuznetsk Basins. In contrast Laxminarayana and Crosdale (1999) showed similar sorption behaviour between dull and bright coals for Bowen Basin coals which is supported by Faiz et al. (1992) on coal samples from the same basin. Similarly, Bustin and Clarkson (1998) concluded from a comparison study between Permian Australian coals and coals from the Western Canadian Sedimentary Basin that there is no definite control on the methane sorption capacity.

Figure 1. Changes in pore space and surface area, chemistry, sorption capacity and moisture content of coal in relation to coalification or maturity.

2 Database and data usage

To verify findings on relationships between gas sorption capacity and coal properties a database with ~1000 entries has been established for this work, containing information on location, age, maturity, proximate and ultimate analysis, sorption capacity and surface area (An et al., 2013; Busch et al., 2003; Cai et al., 2013; Cai et al., 2011; Chalmers and Marc Bustin, 2007; Chen et al., 2017; Crosdale et al., 1998; Day et al., 2008; Dutta et al., 2011; Ettinger et al., 1966b; Faiz et al., 2007; Faiz et al., 1992; Fu et al., 2017; Gasem et al., 2002a; Gasem et al., 2002b; Gensterblum et al., 2013; Gürdal and Yalcin, 2001; Hildenbrand et al., 2006; Hou et al., 2017; Joubert et al., 1973; Joubert et al., 1974; Killingley, 1995; Krooss et al., 2002; Lamberson and Bustin, 1993; Laxminarayana and Crosdale, 1999; Laxminarayana and Crosdale, 2002; Levy et al., 1997; Li et al., 2010; Liu and He, 2017; Manoj, 2016; Nie et al., 2016; Okolo et al., 2015; Pan et al., 2012; Pashin et al., 2004; Pini et al., 2006; Prinz et al., 2004; Reeves et al., 2005; Ryan and Lane, 2002;

Saghafi, 2010; Shan et al., 2018; Tao et al., 2018; Wang et al., 2017; Weniger et al., 2012; Weniger et al., 2010; Yao et al., 2009; Yao et al., 2008; Zhang et al., 2012; Zhao et al., 2016; Zhao et al., 2017; Zheng et al., 2012). Datasets that did not contain information on essential parameters like maturity indicators, age, water content (dry, as received, moisture-equilibrated) or the reporting basis for sorption capacity have been neglected. Sorption capacity, expressed in Langmuir volume, is used on a dry, ash-free basis (daf) throughout this study. Maceral composition is used on a mineral or ash-free basis, so macerals sum up to 100%. Any geological parameters, like burial history or maximum burial depth or mineralogy was considered secondary and not widely reported anyway. It is known that clays can contribute to CH_4 sorption capacity (Ji et al., 2012) of coal. Since clay content and composition is usually not provided, we need to accept this uncertainty, yet, consider it to be low.

In addition, data has been collected to relate structural parameters (e.g. aromaticity, crystallite size and spacing or coal chemistry) to maturity (Commission of the European Communities, 1992; Dun et al., 2013; Ergun, 1968; Everson et al., 2013; Fu et al., 2017; Hattingh et al., 2013; Hirsch, 1954; Li et al., 2015; Li et al., 2013; Lu et al., 2001; Maity and Mukerjee, 2006; Manoj, 2016; Manoj and Kunjomana, 2012; Marques et al., 2009; Nelson, 1954; Roberts et al., 2015a; Roberts et al., 2015b; Rodrigues et al., 2011; Saikia et al., 2009; Sonibare et al., 2010; Van Niekerk et al., 2008). This is important since the development of the coal aromatic/aliphatic structure with maturity is expected to differ for coals of different age, having different original plant input.

It should be noted that all

- All sorption data is reported using Langmuir parameters (Langmuir volume V_L, Langmuir pressure P_L). This is for simplicity reasons and for easy comparison of different datasets. Some authors use an extended version of the classical Langmuir approach by including a term for the sorbed phase density (Gensterblum et al., 2013). This however requires elevated pressures which is not provided by all authors. Others parameterise sorption isotherms using a modified version of the Dubinin-Radushkevich model (Day et al., 2008) which requires a fixed value for the sorbed phase density (e.g. 420 $kg.m^3$ for CH_4). This is in line with the approach by Gensterblum et al. (2013), incorporating the sorbed phase density into the equation with however a fixed value as compared to a value that relates the density to the sorbent and temperature. We therefore use the sorbed phase density independent Langmuir parameters which has been used by most authors.
- Whenever articles were not providing a tabulation of data (either sorption capacity versus pressure or Langmuir parameters), graphs have been digitised, providing the datasets required for fitting the Langmuir equation.
- Vitrinite reflectance data was not provided in all of the studies used in this compilation. Without maturity indicators, the study was discarded. When volatile matter was provided, vitrinite reflectance values were estimated following guidelines by van Krevelen (1993). This approach

was done for <5% of the data presented here and it is assumed that this will not impact the overall outcome of this study.

- The Langmuir volume V_L has been used as the most important parameter for correlation with ultimate and proximate analysis or other factors. In this study it is understood that V_L is independent of temperature, especially for measurements on dry samples. Coal and other microporous sorbents contain a defined number of sorption sites. Filling these sorption sites with the CH_4 depends on temperature. Physisorption is an exothermic process, so sorption sites fill more rapid at low temperature with an increase in pressure. This however does not impact the total amount of sorption sites and since the Langmuir volume is defined as the sorption capacity at infinite pressure, it can be treated as temperature independent over wide temperature ranges (Gensterblum et al., 2014b). However, for moisture containing coals, this is more complicated because the sorption sites are partly occupied by water molecules. The amount of sorbed water molecules at a defined partial pressure depends on temperature such that measurements at different temperatures may have different starting conditions.
- Langmuir pressure P_L is clearly temperature dependent and is therefore less suitable as a correlation factor. Hence comparisons are made at the same or very similar temperature.
- Many studies report the age of the coal formations, however this is not the case for all studies. While the European and North American hard coal deposits are of Carboniferous age and those in the Gondwana coal basins in Brazil, South Africa, India and Australia (exceptions apply) are usually of Permian age, the age question in China is less clear. Here, Tertiary, Jurassic, Permian and Carboniferous coals were deposited, in some instances even within the same basin. Where the age information was not provided, this has been added using information provided on coal mines, coal measures or formation names. This potentially poses some errors however for however <10% of the Chinese datasets.

About 90% of all data relate to coals that are either Permian or Carboniferous in age, with the rest being Jurassic, Cretaceous or Triassic. Since this study aims at statistically meaningful rather than comparing limited datasets, the focus is on Permian and Carboniferous coals only. These form the major coal reservoirs and therefore the major potential coalbed methane reserves worldwide. An overview of these coal basins is provided in Figure 2.

Figure 2. Permian and Carboniferous coal basins and coal areas in the world.

3 Main coal forming eras

There are two main eras of major coal formation in geological history that are fuelling our economies. The first one extends from the Lower Carboniferous (Mississippian) into the Permian, forming most bituminous and anthracitic coals and are mined from subsurface locations down to a depth of more than 1000 m. Given the age of these depositions (Carboniferous coal from about 340 million years (Ma) and Permian coals from about 250 Ma ago), they underwent significant mountain building, subsidence and uplift events that formed 30-40 coal seams of variable geochemical and maceral composition, maturity and permeability (van Krevelen, 1993). During the Carboniferous/Permian coal forming period, two distinct global regions provided the geological and climatic conditions to form the massive coal formations as we know them today: the tropical Carboniferous period produced swamps on the northern hemisphere, stretching from North America and Europe into Siberia and even China. Subsequently, coal formation on the northern hemisphere ceased in the rather dry and cool Permian which led to coal formation on the southern hemisphere, the so called Gondwana continent, combining South America, Africa, India, and Australia and even reaching into China (van Krevelen, 1993). The main difference between the Carboniferous and Permian coal forming periods is climate which has a major control on coal formation. The Carboniferous was warm and humid and the most abundant plant forms were cryptogams (e.g. algae, fungi, mosses, ferns), whereas the Permian was more dry and cool with Glossopteris as the dominating plant form (seed ferns). Corresponding phylogenetic associations are also linked to lignification via increased demand for water (i.e., xylem conduction) because of drier conditions and declining CO_2 partial pressures pCO_2 through the Carboniferous – Permian transition (Sperry, 2003).

The second big era of coal formation starts in Late Cretaceous and peaks in the Tertiary. These are coal formations that are lignite today and that are of limited significance for coalbed methane simply because the thermal maturity to form gas has not been reached. Main plant input that led to the formation of these coals were Angiosperms (trees, palms etc). We will not discuss this era much further in the context of this study but name it for completeness.

4 Coal sorption and relation to coal properties

4.1 Moisture content and maceral composition

Equilibrium moisture content is obtained in the laboratory following strict procedures (ASTM, 2018). It is considered that the equilibrium moisture state corresponds closest to reservoir conditions where the coal pore system is fully water saturated. As such, equilibrium moisture strongly correlates with the accessible pore space, which varies with coal maturity, as shown in Figure 3. This parabolic trend is directly related to the schematic behaviour illustrated in Figure 1, where an increase in maturity leads to the formation of oil droplets which is followed by cracking of these oil droplets at ~1.3 % VRr. At VRr of about 1.1 % polyaromatic units (also called basic structural units) as well as crystallites form, which build up zones of oriented aromatic clusters or molecular orientation domains (Prinz and Littke (2005)). This leads to a

general increase in micropores but also to an increase in water-accessible micropores, hence equilibrium moisture. In Figure 3, there seems to be a similar behaviour for Permian and Carboniferous coals. It should however be noted that water cannot access pores smaller than about 0.4 nm, also termed ultra-micropores (Prinz and Littke, 2005). This is likely due to clustering of water molecules (molecule size ~0.28 nm, (Nishino, 2001)). It should also be noted that we see some gaps in data, especially for very low maturity coals (<0.3% VRr) or between 2 and ~2.7% VRr. It is well known that for very low maturity coals water content can be significantly higher than what is indicated in Figure 3 (Bongers et al., 1998).

Figure 3. Equilibrium moisture content versus vitrinite reflectance VRr using the database compiled for this study. It is seen that moisture content decreases to about 1.3-1.5% VRr, after which an increaser is indicated. No difference between Carboniferous and Permian coals circles is observed.

As mentioned earlier, different studies postulate an impact of maceral composition on methane sorption capacity, where the main control can be vitrinite (Crosdale et al., 1998; Laxminarayana and Crosdale, 2002) or inertinite (Ettinger et al., 1966b). Here we show that maceral composition has no impact on the sorption capacity of either dry or moisture-equilibrated coals (Figure 4).

Figure 4. Vitrinite (mmf) content versus Langmuir volume for dry and moisture-equilibrated samples.

4.2 Langmuir volume of Permian and Carboniferous coals

Figure 5 shows the difference in Langmuir sorption between Permian and Carboniferous coals in relation to coal rank and for three different moistures state, namely dry, as-received and moisture-equilibrated (moist). The as-received moisture state is undefined and it typically involves a measurement on a sample that was allowed to dehydrate for unspecified amounts of times in unspecified laboratory or core store environments. As a consequence, the moisture content varies between dry and fully water-saturated. For the dry and moist samples we assume that sample pre-treatment followed comparable standards, hence that starting conditions are similar.

For dry coals, clear differences between the two sample sets can be observed (Figure 5), whereby Permian coals adsorb 1.5 to 2 times more methane than Carboniferous coals, independent of maturity. Both datasets may indicate a parabolic ("u-shaped") trend with maturity as observed previously (Busch and Gensterblum, 2011), similar to the one discussed for equilibrium moisture in Figure 3. This trend is however not clear by and we found a linear fit to be most suitable, based on the data only and especially for Carboniferous coals. It also becomes apparent that sorption capacity for Carboniferous coals vary between 10 and 35 $m^3.t^{-1}$ only, while values for Permian coals vary between 15 and about 80 $m^3.t^{-1}$. When

comparing with the as-received samples we see a similar behaviour of generally lower sorption capacities for Carboniferous compared to Permian coals. This difference is however not as clear as for the dry samples and we find lower or similar values for Permian than for Carboniferous coals at comparable maturity. This can of course relate to differences in moisture levels which however remains unclear. But we can state that, given the difference in data points, the spread in values is bigger for Permian compared to Carboniferous coals.

Lastly, when comparing moist coals, no obvious differences in sorption capacity is observed for both datasets. This is relevant for reservoir behaviour since a certain water-saturation is expected in coalbeds. Water-saturated Permian and Carboniferous coals show no difference in sorption capacity and water can only fill pores of sizes >~1 nm due to clustering at the entrance of the pore (Prinz and Littke, 2005). Consequently, the sorption difference between dry Permian and Carboniferous coals relates to the surface area associated with pores <~1 nm but larger than the size of methane molecules which is 0.3751 nm (Kurniawan et al., 2006) but it is also the size of pores providing most of the coal internal surface area (Prinz and Littke, 2005). Figure 6 shows data for specific surface area determined using CO_2 low pressure sorption (CO_2 LPS) on dry Permian and Carboniferous coals versus Langmuir volume on dry coal samples. CO_2 LPS probes the surface area of micropores. Sorption capacity generally increases with an increase in specific surface area however no clear relationship is identified with coal rank. Even though data points for Carboniferous coals are limited (n=8), it is obvious that surface area is significantly lower than for Permian coals (n=23), on average about 60%. This coincides with the average difference in Langmuir volume between the two datasets (61%) and clearly demonstrates that sorption capacity on dry coal is directly related to micropore surface area and that this surface area is significantly higher in Permian than in Carboniferous coals. Using a statistically more relevant set of data and to strengthen the argument of Permian coals having higher surface areas than Carboniferous coals, Figure 6 (right) shows CO_2 specific surface area (SSA) versus maturity, again with a difference between the two datasets of 62% at similar average SSA values.

Figure 5: Langmuir volume V_L as a function of vitrinite reflectance VRr for dry (A), as received (B) and moisture-equilibrated (C) graphs. Clear differences are shown between Carboniferous and Permian samples which is increasing with a decrease in water content. For the dry samples, V_L values for Permian coals are almost twice as high as for the Carboniferous coals and an indication for a u-shaped trend in sorption capacity is indicated for both datasets. As received (a.r.) samples show a similar behaviour than the dry samples with generally higher sorption capacities for Permian compared to Carboniferous coals. For moisture-equilibrated samples no clear difference can be observed and sorption capacities seem to increase with increasing maturity as already indicated by (Prinz and Littke, 2005).

Figure 6: CO_2 specific surface area in relation to Langmuir volume (left) and vitrinite reflectance (right) for dry Carboniferous and dry and as received Permian coal samples.

Higher SSA is expected to be related to the micropore structure and possibly composition of the functional groups. Focusing on the chemical composition of the Permian and Carboniferous samples suggests oxygen content as a possible control on sorption capacity. Figure 7 shows that oxygen contents in Permian coals are generally higher than in Carboniferous coals (~62%), and that V_L generally decreases exponentially with an increase in oxygen content. We do not observe a direct control of oxygen content on the difference between Permian and Carboniferous coals that is related to carboxylic and hydroxylic functional groups. Such a control requires a more detailed analysis based on an even larger data base.

Figure 7: Oxygen content versus vitrinite reflectance (A) and Langmuir volume (B) of dry Permian and Carboniferous coals.

4.3 Coal Structural Properties

As discussed earlier micropore surface areas for pore sizes <1 nm differ significantly between Permian and Carboniferous coals. This difference could be reflected in coal structural parameters as determined using X-ray diffraction, Raman, and FTIR spectroscopy. These parameters are average lateral size (La), stacking height (Lc), and interlayer spacing (d_{002}) of crystallite structures as well as the relative aliphatic/aromatic compounds of coals. The interlayer spacing d_{002} between the crystals might be an important control on surface area, providing access to methane to sorb. Figure 8 shows that d_{002} roughly equals the size of a methane molecules (3.4 to 3.8 Å) and values generally increase linearly with an increase in VM, corresponding to a decrease in coal maturity. No major difference is observed between the two datasets and the behaviour with maturity is largely similar. As evident from Figure 8, the CH_4 kinetic diameter exceeds the crystallite interlayer spacing which suggests that even if there would be a difference between Carboniferous and Permian coals, this effect would be unobserved. In a similar manner for stacking height and crystallite area, no difference was observed.

Figure 8. Crystallite interlayer spacing versus volatile matter. Here volatile matter acts as maturity indicator, whereby lower values indicate higher maturity. Kinetic diameter for CH_4 was taken from Jacops et al. (2017).

In the following we investigate the contribution of aromaticity on Langmuir volume for Permian and Carboniferous coals. Figure 9 shows the relationship between VM and aromaticity for the two datasets; Carboniferous coals are clearly more aromatic than Permian coals across the VM (maturity) range and aromaticity linearly decreases with VM. Higher aromaticity at lower sorption capacity for Carboniferous coals contradicts findings of Fu et al. (2017) who showed a significant increase in methane sorption capacity with aromaticity for dry Permian coals.

Figure 9: Aromaticity versus volatile matter content (as maturity indicator), showing higher aromaticity for Carboniferous coals at similar volatile matter content (or maturity) than the Permian coals.

4.4 Langmuir Pressure

Differences in the chemistry of sorption sites are expected to impact sorption energies. The Langmuir Pressure P_L is an indirect measure of sorption energy whereby low values indicate high energies and vice versa. Furthermore, sorption is an exothermic process, so with an increase in temperature an increase in P_L can be expected. Figure 10 shows P_L values for dry and moist coal samples at different temperatures. In general, all values are below 4 MPa and no significant difference between Permian and Carboniferous coals can be observed. For dry samples (Figure 10), values are generally lower than 2MPa with the exception of measurements performed at VRr ~0.8 to 1.2%. Here, P_L values increase to 5-6 MPa for temperatures <322 K and even to 14 MPa for temperatures in excess of 342 K. The latter is not surprising since sorption is exothermic but the peak around VRr~1% is obvious. This coincides with the formation of oil droplets in the micropores whereby an important fraction and potentially high-energy sorption sites in the micropores might become blocked. Consequently, methane sorbs either on liquid hydrocarbons or on lower energy sorption sites in the mesopores. A similar observation is made for moist samples with peak P_L values around 0.8 to 1.5% VRr. Within this range, there seems to be a trend of Carboniferous having higher P_L values than Permian coals.

Figure 10: Langmuir Pressure P_L versus vitrinite reflectance VR for dry and moisture-equilibrated coals. Closed symbols correspond to Permian and open symbols to Carboniferous coals.

5 Coal Pore Shape and Connectivity

Not only coal internal surface area or the composition of functional groups are of importance but also pore shape (spherical, ellipsoid, slit-shaped etc.), pore connectivity, and alignment, which might differ for coals of different rank, degree of compaction, age, and maceral composition.

The surface area of coal is largely associated with its micropore system with sizes <2 nm. Within this microporosity, pores between 0.5-0.6 nm in size are dominant (Walker et al., 1981). It has been shown that about 95 % of the total internal surface area relates to these pore sizes, comprising about 80% of the internal free volume in a high-rank coal in comparison to 50-60% in a low rank coal (Gorbaty et al.,

2013). The micropore structure of coal is still not understood in detail due to the lack in resolving such small structures by most analytical techniques.

Similarly, the geometry and connectivity of micropores and the connectivity to larger pores have not firmly been established. The pore geometry observed by most experiments demonstrated aspect ratios (length/width) of <10 (Giffin et al., 2013; Radovic et al., 1997). Conical and slit-shaped micropores are thought to be dominant throughout the size scale (Cardott and Curtis, 2018; Radovic et al., 1997). The micropore network exhibits numerous constrictions or narrow throats which limit the accessibility of the gas molecule to the micropore space, known as the molecular sieve effect (Mahajan, 1982; Mahajan, 1991; Marsh, 1987; Walker and Mahajan, 1993; Walker et al., 1981). An energy barrier need to be overcome for gas to enter a micropore. Nelson and Walker (1961) and Nandi and Walker Jr. (1970) found that the activation energy of methane is lower than for N_2, but higher than for CO_2, which corresponds to the relative sorption capacity of the three gases, namely CO_2>CH_4>N_2. Thus, CO_2 is able to access a larger fraction of micropores. The significantly higher surface area provided by low pressure CO_2 sorption at 273 K comparted to N_2 at 77 K, confirms that during CO_2 low pressure sorption ultramicroporous (<0.4 nm) can be accessed that are not accessible to N_2 at 77 K. Bae et al. (2009) estimated that the volume of the micropores accessible to CO_2 but inaccessible to CH_4 is 13% and 17% of the total micropore volume for the two coal samples.

Anderson et al. (1997) and Radovic et al. (1997) showed by using by ^{129}Xe nuclear magnetic resonance spectroscopy, that micropore connectivity is rank dependent. Tortuosity of the micropore network is higher in coals with a carbon content >88%. Micropores are more open to large pore clusters, and are less constricted in low-rank compared to high-rank coals. There are indications that the pore space of anthracite is better connected than medium-volatile bituminous coals. The interconnected but constricted micropore system is mainly related to the macromolecular structure. Although several chemical and physical coal structures have been proposed (Given et al., 1986; Hirsch, 1954; Narkiewicz and Mathews, 2008; Shinn, 1984; Spiro, 1981), only few describe the formation of micropores in the cross-linked, three-dimensional spiral macromolecular network. As a consequence, the micropore structure can only be inferred qualitatively from the existing knowledge on coal macromolecular structure.

Chemically, the macromolecular is made of numerous resembled condensed aromatic units with aliphatic side chains bridging to functional groups. The size, orientation and spacing of condensed aromatic units may provide information on the shape and size of micropores. It is known that the condensed aromatic units tend to stack parallel to each other, but orientation and planarity are imperfect because of the presence of functional groups and aliphatic portions (Millward, 1979). It is generally accepted that anthracites are well ordered, bituminous coal have some orientation, low-rank coals have a more or less random ordering (van Krevelen, 1993). The structural alignment of coal was quantitatively described by Mathews and Sharma (2012). They demonstrated that lignite and bituminous coals show similar

orientations of 24% and 22% respectively, while a low-volatile bituminous coal shows slightly larger (39%) alignment with extensive alignment (65%) in the case of anthracite coal.

Evidently, anthracites have larger condensed aromatic unit sizes of >1 nm and less interlayer spacing <0.35 nm than low-rank coal (Oberlin et al., 1980; Rouzaud and Oberlin, 1990; Sharma et al., 2000). This implies that anthracites are likely to possess more regular flattened (slit-shape) micropores of smaller size (Deurbergue et al., 1987). With decreasing coal rank, the aromaticity decreases while the number and length of side chains and functional groups increases and the parallel orientation is distorted from planarity by the aliphatic moieties and heteroatoms which are directed into the spatial regions between the slightly irregular condensed aromatic units (Wertz and Bissell, 1994). These result in a slightly decrease in the average layer size and increase of interlayer spacing (Oberlin et al., 1980; Rouzaud and Oberlin, 1990; Sharma et al., 2000). On the one hand, micropores between the layers become larger and more irregular in shape. On the other hand, "new" micropores are formed caused by the intertwining of aliphatic side chains and functional groups. This is evidenced by the X-ray diffraction data where pore structures of similar size (i.e. 0.6 nm) had different chemical compositions, which were tentatively assigned to aromatic and aliphatic regions of the coal (Tsiao and Botto, 1991). It is reasonable to infer that low-rank coals have a relatively open and dendritic structure with well-developed micropore systems due to the large amount of various functional groups. Thus, the high orientation of lamellae and the increase in the population of oxygen surface groups are responsible for the large number of micropores and high surface area in the high rank and low rank coals, respectively.

Although no work has been done to systematically analyse differences in coal age, it is reasonable to infer that Permian coals may pose a larger amount of micropores with sizes larger than 0.4 nm due to their higher oxygen contents and lower aromaticity than that of Carboniferous coals, which may result in higher surface area and higher methane sorption capacity.

6 Statistical analysis of coal ultimate, proximate, surface area and Langmuir parameters

For statistical analysis we used compositional bi-plots that are based on the centred log-ratio (clr) transformation (Jolliffe and Cadima, 2016; Karacan and Olea, 2018). The bi-plots represent a 2-D singular value decomposition (SVD), where the individual data points are represented as dots and the variables are represented as rays (Jolliffe and Cadima, 2016). The length of a ray is proportional to the standard deviation of the variable it represents. If two rays are near each other, the variables might be highly associated. If rays are orthogonal, the two simple log-ratios are uncorrelated. In general, PCA examines relationships of variables; it can be used to reduce the number of variables in regression and clustering, for example. Each principal component in PCA is the linear combination of the variables and gives a maximized variance.

Figure 11 shows the bi-plots of the coal proximate and Langmuir properties (VRr, VL, inertinite, vitrinite and volatile matter) as well as oxygen and specific surface area data for dry and moist samples respectively. Each bi-plot shows the data for Permian and Carboniferous coals separately, while the rays in its length and direction represent the entire dataset. We split the data into two plots for both, the dry and moisture-equilibrated samples, mainly because of the different data origin. There are no or only few consistent datasets that contain proximate, ultimate, Langmuir and surface area data. The plots were generated using the Principal Component Analysis (PCA) module of the software Origin. The principal components shown in these plots, which are valid for the entire sample set, represent 80% and 83% of the cumulative variance for the dry as well as 60% and 90% for the moist sample dataset. Each point in the plot represents a sample where each of the principle components were available. This limits the sample density in comparison to the binary plots in Figure 3 to Figure 10. In Figure 11A and C vitrinite and inertinite as well as VRr and VM show opposite direction. This is because when vitrinite values are high, inertinite values are low and vice versa. The same holds for VRr and VM.

Figure 11A shows a clear relationship between maturity and V_L for dry coals but no relationship with maceral composition, in line with earlier findings of this study. Given that dots for Carboniferous and Permian coals overlap, these relationships are valid for both datasets. In Figure 11B CO2SSA and V_L are related as well as VRr and Oxygen. Here, Carboniferous and Permian coals differ substantially and two different data clouds can be observed. This may be due to the obvious difference in absolute values for both datasets (Fig 6, Fig7). For moist coals in Figure 11C we see much weaker correlations between V_L and maturity and rather random data point for the two datasets. As expected, equilibrium moisture contents correlate with maturity and maceral composition is widely unrelated, as indicated in Fig. 4. Figure 11D shows a weak correlation of parameters as well, however based on a low data density. Here, V_L and maturity seem to have a correlation which is not indicated for the more proximate/Langmuir property data in Figure 11C.

Figure 11: Bi-plots for proximate and Langmuir parameters (left) as well as ultimate, Langmuir and surface area properties (right) of dry (A and B) and moisture-equilibrated (C and D) coals.

7 Relation to original plant material

We demonstrated that sorption effects are complex and difficult to resolve in most types of kerogen as a consequence of heterogeneities in composition, origin, age, and burial history (thermal maturity). Such difficulties are especially prohibitive among gas-rich coalbeds (Zhang and LeBoeuf, 2009) because no consistent (non)linear correlations are apparent between sorption of methane in coals and their maturation state (Harpalani et al., 2006) for coal-bearing provinces on a worldwide scale (Bustin and Clarkson, 1998). Even so, several basin-specific studies demonstrate increasing gas sorption alongside

vitrinite content (Zhang and LeBoeuf, 2009) that hints at the importance of higher woody plant tissues vis-à-vis specific surface area on coal formation dynamics.

Numerous studies indicate sorption characteristics of hydrophobic organic molecules, such as methane, in coals are related to micropore volume access (Gensterblum et al., 2014a; Prinz and Littke, 2005) that in turn is related to maceral distributions (Busch and Gensterblum, 2011; Milewska-Duda, 2000). Although there is some support for methane sorption on microporous aromatic structures of diverse coals (Gensterblum et al., 2013), aromaticity alone is a weak predictor of hydrophobic organic molecule sorption (Figure 9) as is maceral composition (Figure 4). Instead, the results of former studies (Busch and Gensterblum, 2011; He et al., 2012b; Wang et al., 2007) highlight the importance of biopolymer ultrastructure on methane sorption, regardless of type or rank (Figure 5). For instance, studies of isolated biopolymers suggest that lignin is a stronger, more consistent determinant for organic sorption as compared to other macromolecules (Ran et al., 2013) and inorganic minerals (MacKay and Gschwend, 2000). As such, it is logical to focus on the relationship(s) shared between methane sorption and lignin characteristics across our database of Paleozoic (Carboniferous and Permian) coals with complementary physiochemical differences (see Database and Data Usage section).

In complement to many previous studies showing relationships between sorption capacity and maceral composition or coalification, we show similar or even stronger relationships exist between sorption capacity and the stratigraphic age of Paleozoic coal samples (Figure 5). Indeed, there is clear evidence showing partially water-saturated and dehydrated Permian 'Gondwana' coals adsorb more methane than Carboniferous coals, independent from maceral composition or maturity.

7.1 Coal composition

Coals are characterized by heterogeneous organic matter composition due to selective preservation of differing plant-type and tissue inputs (Brochard et al., 2012). Despite such compositional heterogeneities, the organic matter in coals is composed of just three major macerals (Scott, 2002): vitrinite, liptinite, and inertinite. Vitrinite is the dominant maceral in most humic coals, and is considered to originate from aromatic coalified lignin (Hatcher et al., 1990; Taylor et al., 1998). In contrast, lipitinite originates from more aliphatic (i.e., acyclic) molecules, such as cutin and cross-linked (hydroxy)fatty acids (Scott, 2002). Inertinite (fusinite) is equivalent to charcoal from oxidized (burnt) plant tissue (Hatcher et al., 1990; Taylor et al., 1998). Considered together, each of these macerals are characteristically produced from decaying plant tissues accumulated in wetlands, which were converted to an organic-carbon-rich rock through high temperature–pressure sedimentary processes.

Although coals show marked heterogeneities in organic carbon composition, on average coals contain at least 50% lignin or direct lignin derivatives (i.e., vitrinite) regardless of thermal history (Hatcher and Lerch, 1991). Vitrinite also contains other significant high-molecular-weight biopolymers, such as condensed tannins, which, like natural lignin, contain many phenolic structures (c.f., Figure 12, Figure 13).

Cellulosic derivatives are of limited importance in coal due to microbial degradation of β-linked hexose (saccharide) bonds. Even so, micropore structures can remain intact despite significant losses of inceptive cell wall biomolecules viz. (poly)saccharides (Hatcher and Lerch, 1991) because of the close association between cellulosic and lignin structures of <1.5 nm diameter during decomposition (Adani et al., 2010; Papa et al., 2014).

Figure 12: Important lignin oxidation derivatives in monomeric and dimeric (inset) forms (Hedges and Mann, 1979). Generally, p-hydroxyl base units occur in all higher (vascular) plants, as well as many 'primitive' species of lower plants (e.g., protracheophytes, Figure 14). In contrast, V base units are synthesized by just higher vegetation species. S base units are derived from angiosperms and ferns, although ferns contain much less abundant S-to-V base units as compared to angiosperms. Cinnamyl base units are synthesized by plants with non-woody growth forms and leaf tissue (Goñi and Hedges, 1992).

Figure 13: Selected lipid biomarker structures, common names, and dominant biomass source(s) (Peters et al., 2005). Methylphenanthrenes are characteristically petroleum-derived biomarkers, although their inceptive sources are non-specific.

7.2 Gas sorption in coals

Previous studies suggest that the sorption of key gases, such as methane, in coals is not linked to chemical (ad)sorption on organic molecules (Hatcher and Clifford, 1997) or inorganic minerals (MacKay and Gschwend, 2000) but instead to stearic (physical) factors (Zhang and LeBoeuf, 2009) related to macromolecular structure (Guo et al., 2017). For instance, earlier studies suggest that the sorption capacities of typical coals decrease with moisture content because of decreasing pore sizes and biopolymer swelling (Chen et al., 2005; Zhang and LeBoeuf, 2009) together with changes in corresponding polarity (Chen et al., 2005; Zhang and LeBoeuf, 2009). Further, sorption nonlinearities increase with aromatization and lignin condensation (He et al., 2012a) in a manner suggestive of hole-filling processes (e.g., gas sorption) within micropores of the aromatic domain (Keiluweit et al., 2010; Magill et al., 2015; Tang and Weber, 2006). Withal the observed thermodynamic characteristics of bulk coal have a direct dependence on its associated biopolymeric composition, as defined by plant lignin (He et al., 2012a; Zhang and LeBoeuf, 2009).

7.3 Lignin

Lignin is one of the most abundant bio(macro)molecules on earth, where it accounts for almost 30% of total biospheric organic carbon. In its native unaltered form, lignin occurs as an extensively phenolic (aromatic) branched three-dimensional biopolymer, synthesized from oxidative radicalization of three simple alcohol base units (monolignols): coniferyl-, coumaryl-, and sinapyl alcohol. Respective

monolignols are incorporated by plants into recalcitrant lignin aromatic core structures as complementary phenylpropane monomers – namely p-hydroxyphenyl (H), vanillyl (V), and syringyl (S) – linked by polydispered C–C and C–O (ether) bonds. In addition to dominant lignin monomers, other minor monomers such as cinnamyl (C) base units also assist in lignification of herbaceous, non-woody plant tissues (Figure 12). Although the mechanisms of lignification are conserved in contemporary plants (Radovic, 1997), relative abundances of lignin monomers and bond types show marked differences among plant types and tissues (c.f., below) that lead to substantial differences in ultrastructure of lignin itself (Sarkar et al., 2009).

7.3.1 Lignin monomers

The monomeric composition of lignin differs among plant types, which in turn influences (sub)micropore structure in coals. Generally, gymnosperm (conifer) lignin contains abundant V base units with limited (<5%) H base units of total lignin monomers. Other major (sub)groups of higher vegetation, namely pteridophytes (e.g., ferns), also contain abundant V base units with additional, though variable, occurrences of S base units (Smoot and Smith, 2013). Lignin in angiosperms also contains a combination of V and S base units (DiMichele and Aronson, 1992); however, available molecular and fossil data suggest that this clade did not emerge until the mid-Mesozoic (Weng et al., 2008), about 200 Ma. In contrast, C base units are characteristic of herbaceous (non-woody) plant tissues in all tracheophytes (Figure 12).

Lignin structure is not determined by just base unit distribution, and likewise depends on inter-unit bonds created during plant lignification. The commonest lignin motif incorporates ether alkyl-aryl (β–O–4) linkages across aromatic rings. Other important, though less common, motifs also incorporate condensed β–β, β–5, and 5–5´ linkages (Figure 12). Even so, condensed bond frequencies can differ among plant types (DiMichele and Aronson, 1992). For instance, aforementioned β–O–4 bonds dominate among gymnosperms and lead to more oxygen-rich, caged (C–C [cross]linked) biopolymeric structures as compared to among pteridophytes or angiosperms, in which lignin creates a straight (linear) structure as a consequence of S base units with multiple ortho methoxy groups (see Figure 12) Such higher oxygen contents are also illustrated in Figure 7 where a shift to higher Langmuir volumes can be observed, indicating higher capacities for coals enriched in oxygen-containing functional groups.. Indeed, the major structural differences apparent between G-dominated (e.g. gymnosperms), G–S (e.g. pteridopytes), and S-dominated lignin are consequent to methoxy groups at the 5-position of S base units (Figure 12, Figure 14). As such, β-ether bond frequencies of lignin increase with increasing proportions of S-to-G base units (Jex et al., 2014). Lignin structural differences are important because β–O–4 bonds are much less stable than condensed biphenyl 5–5´ bonds, which are only present between G base units (Jex et al., 2014). Previous studies also suggest that the initial 3-dimensional biopolymer structure of lignin influences sorption of key gases in coal (Busch and Gensterblum, 2011; Magill et al., 2015) because it defines average micropore volume and their accessibility (He et al., 2012b).

7.4 Paleozoic evolution and dominance among plants

The impact of floral tissue composition on coal during progressive maturation requires in-depth knowledge about the rise of lignified tissues with respect to overarching plant diversification (evolution) through Carboniferous (warm and humid) to Permian (cool and dry) paleoclimate conditions. Upper Carboniferous (323–299 Ma) vegetation communities were well-developed throughout (sub)tropical Gondwanaland, but had low morphologic and taxonomic diversity (Cleal et al., 2012). These communities were dominated by just three key plant types (clades): lycopsids, ferns, and less common seed-bearing plants such as early ginkophytes and Cordaites (i.e., early gymnosperms) (Banasiak, 2014). Lycopsids are represented by giant lepidodendrid (scaly) trees, which dominated biomass input to wetlands, including peatland (DiMichele et al., 2001). Importantly, previous studies suggest that Upper Carboniferous species of lycopsids and ferns alike contained lignin with abundant V base units and $<10\ \mu g\ g^{-1}$ of S base units (Bateman et al., 1998; Logan and Thomas, 1985).

The dominance of Carboniferous woody pteridopytes (ferns) shifted towards seed-bearing plants around 300 Ma as a consequence of Permo-Carboniferous climate change (Banasiak, 2014). This shift in dominance resulted in much higher-diversity plant communities with increasing proportions of Glossopterid (seed) ferns and highly productive early gymnosperms (DiMichele et al., 2001; Logan and Thomas, 1987). In contrast to coeval lycopsids, seed ferns and Cordaites contained V and C base units without S base units (DiMichele and Aronson, 1992). As such, the respective abundance of dominant lignin monomers, and therefore structure (Donaldson, 2001), in sedimentary geologic archives should follow alongside evolutionary patterns of land plants (Logan and Thomas, 1985; Novo-Uzal et al., 2012).

Figure 14: Plant evolutionary (phylogeny) patterns amid the Paleozoic–Mesozoic transition (Laskar et al., 2012; Pittermann, 2010), ca. 251 Ma. Carboniferous (dark lavender) vegetation communities were dominated by prominent lycophytes, seed ferns, and ferns. Permian (light lavender) communities included dominantly gymnosperms and ferns, which have different lignin compositions and biopolymeric structures as compared to all lycophytes (DiMichele and Aronson, 1992; Sperry, 2003; Weng et al., 2008). ‡Extinct lineage. V, vanillyl; V+S, vanillyl plus syringyl; S, Silurian; D, Devonian; C, Carboniferous; P, Permian; Tr, Triassic; J, Jurassic.

8 Conclusions

We have shown that the primary factor controlling gas sorption in coals is the period of coal deposition with Permian coals sorbing significantly higher amounts than Carboniferous coals. This difference is substantiated in clear differences in micropore surface area scaling linearly with Langmuir volume, higher oxygen contents in Permian coals but lower aromaticity at comparable maturity. Secondary physicochemical controls on CH_4 sorption are water content. For fully water-saturated coals, the

difference between Permian and Carboniferous coals is not evident. Water is filling meso and macropores as well as some larger micropores. This prohibits gas access to the smaller micropores that control gas sorption. Another secondary control is coal maturity which mainly relates to the formation of liquid hydrocarbons in the micropores with an increase in coal maturity. This formation peaks at a vitrinite reflectance of ~1.1 to 1.3% which shows a minimum in sorption capacity for Carboniferous and Permian coals. Upon maturity increase and cracking of liquid hydrocarbons, successively more micropore volume is getting accessible for gas sorption. We did not identify any control of maceral composition on gas sorption capacity of coals. Furthermore, studying the available literature on pore geometry and pore connectivity did not reveal any control on CH_4 sorption but information is limited and might be a topic for future research. We relate the differences in sorption capacity of Permian and Carboniferous coals to the plant tissue structure at the (sub)micropore scale that relates to macromolecular architecture as defined through biopolymers, especially lignin, amid the coalification process. This macromolecular architecture is conserved even after maturation and even in coals with high thermal maturity. We find that the macromolecular structure and chemical properties (i.e., polarity or hydrophobicity) of lignin are likely to influence methane sorption in coals. Major diversification events during plant evolution at the Carboniferous-Permian transition, especially the rise of Euphyllophytes (e.g., conifers), had a direct influence on methane sorption in coals because of associated changes in lignin abundance, composition and 3D structure at the micropore scale. Future studies about CBM will benefit from consideration of the age and plant communities, in addition to more conventional indices of thermal maturity (VRr) etc., when identifying patterns in methane sorption capacities or/and identifying potential locations with economic viability.

9 References

Adani, F., Papa, G., Schievano, A., Cardinale, G., D'Imporzano, G. and Tambone, F., 2010. Nanoscale structure of the cell wall protecting cellulose from enzyme attack. Environmental science & technology, 45(3): 1107-1113.

An, F.-H., Cheng, Y.-P., Wu, D.-M. and Wang, L., 2013. The effect of small micropores on methane adsorption of coals from Northern China. Adsorption, 19(1): 83-90.

Anderson, A.S., Hatcher, G.P. and Radovic, L., 1997. Effects of surface chemistry on the porous structure of coal.

ASTM, 2018. ASTM D1412 / D1412M, Standard test method for equilibrium moisture of coal at 96 to 97 percent relative humidity and 30°C.

Bae, J.-S., Bhatia, S.K., Rudolph, V. and Massarotto, P., 2009. Pore accessibility of methane and carbon dioxide in coals. Energy & Fuels, 23(6): 3319-3327.

Banasiak, A., 2014. Evolution of the cell wall components during terrestrialization, 83, 349-362 pp.

Bateman, R.M., Crane, P.R., DiMichele, W.A., Kenrick, P.R., Rowe, N.P., Speck, T. and Stein, W.E., 1998. Early evolution of land plants: Phylogeny, Physiology, and Ecology of the Primary Terrestrial Radiation. Annual Review of Ecology and Systematics, 29(1): 263-292.

Bongers, G.D., Jackson, W.R. and Woskoboenko, F., 1998. Pressurised steam drying of Australian low-rank coals: Part 1. Equilibrium moisture contents. Fuel Processing Technology, 57(1): 41-54.

Brochard, L., Vandamme, M., Pellenq, R.J.M. and Fen-Chong, T., 2012. Adsorption-Induced Deformation of Microporous Materials: Coal Swelling Induced by CO2–CH4 Competitive Adsorption. Langmuir, 28(5): 2659-2670.

Busch, A. and Gensterblum, Y., 2011. CBM and CO2-ECBM related sorption processes in coal: A review. International Journal of Coal Geology, 87(2): 49-71.

Busch, A., Gensterblum, Y. and Krooss, B.M., 2003. Methane and CO2 sorption and desorption measurements on dry Argonne premium coals: Pure components and mixtures. International Journal of Coal Geology, 55(2-4): 205-224.

Bustin, R.M. and Clarkson, C.R., 1998. Geological Controls on coalbed methane reservoir capacity and gas content. International Journal of Coal Geology, 38: 3-26.

Cai, Y., Liu, D., Pan, Z., Yao, Y., Li, J. and Qiu, Y., 2013. Pore structure and its impact on CH4 adsorption capacity and flow capability of bituminous and subbituminous coals from Northeast China. Fuel, 103: 258-268.

Cai, Y., Liu, D., Yao, Y., Li, J. and Qiu, Y., 2011. Geological controls on prediction of coalbed methane of No. 3 coal seam in Southern Qinshui Basin, North China. International Journal of Coal Geology, 88: 101-112.

Cardott, B.J. and Curtis, M.E., 2018. Identification and nanoporosity of macerals in coal by scanning electron microscopy. International Journal of Coal Geology, 190: 205-217.

Chalmers, G.R.L. and Marc Bustin, R., 2007. On the effects of petrographic composition on coalbed methane sorption. International Journal of Coal Geology, 69(4): 288-304.

Chen, B., Johnson, E.J., Chefetz, B., Zhu, L. and Xing, B., 2005. Sorption of polar and nonpolar aromatic organic contaminants by plant cuticular materials: Role of polarity and accessibility. Environmental Science & Technology, 39(16): 6138-6146.

Chen, S., Tao, S., Tang, D., Xu, H., Li, S., Zhao, J., Jiang, Q. and Yang, H., 2017. Pore structure characterization of different rank coals using N2 and CO2 adsorption and Its effect on CH4 adsorption capacity: A case in panguan syncline, Western Guizhou, China. Energy & Fuels, 31(6): 6034-6044.

Cleal, C.J., Uhl, D., Cascales-Miñana, B., Thomas, B.A., Bashforth, A.R., King, S.C. and Zodrow, E.L., 2012. Plant biodiversity changes in Carboniferous tropical wetlands. Earth-Science Reviews, 114(1-2): 124-155.

Commission of the European Communities, 1992. Characterisation of coal and coal products by solid-state nuclear magnetic resonance spectroscopy to aid conversion processes, EUR14069, Luxembourg.

Crosdale, P.J., Beamish, B.B. and Valixa, M., 1998. Coalbed methane sorption related to coal composition. International Journal of Coal Geology, 35: 147-158.

Day, S., Sakurovs, R. and Weir, S., 2008. Supercritical gas sorption on moist coals. International Journal of Coal Geology, 74(3-4): 203-214.

Deurbergue, A., Oberlin, A., Oh, J.H. and Rouzaud, J.N., 1987. Graphitization of Korean anthracites as studied by transmission electron microscopy and X-ray diffraction. International Journal of Coal Geology, 8(4): 375-393.

DiMichele, W.A. and Aronson, R.B., 1992. The Pennsylvanian-Permian vegetational transition: a terrestrial analogue to the onshore-offshore hypothesis. Evolution, 46(3): 807-824.

DiMichele, W.A., Pfefferkorn, H.W. and Gastaldo, R.A., 2001. Response of Late Carboniferous and Early Permian plant communities to climate change. Annual Review of Earth and Planetary Sciences, 29(1): 461-487.

Donaldson, L.A., 2001. Lignification and lignin topochemistry—an ultrastructural view. Phytochemistry, 57(6): 859-873.

Dun, W., Guijian, L., Ruoyu, S. and Xiang, F., 2013. Investigation of structural characteristics of thermally metamorphosed coal by FTIR spectroscopy and X-ray diffraction. Energy & Fuels, 27(10): 5823-5830.

Dutta, P., Bhowmik, S. and Das, S., 2011. Methane and carbon dioxide sorption on a set of coals from India. International Journal of Coal Geology, 85(3-4): 289-299.

Ergun, S., 1968. X-ray studies of coals and carbonaceous materials, US Department of the Interior - Bureau of Mines, Bulletin 648, 40 pages.

Ettinger, I., Chaplinsky, A., Lamba, E. and Adamov, V., 1966a. Natural factors influencing coal sorption properties - III Comparative study of carbon dioxide and methane on coal. Fuel, 45: 351-367.

Ettinger, I., Eremin, B., Zimakov, B. and Yanovskaya, M., 1966b. Natural factors influencing coal sorption properties I Petrography and the sorption properties of coals. Fuel, 45: 267-274.

Everson, R.C., Okolo, G.N., Neomagus, H.W.J.P. and dos Santos, J.-M., 2013. X-ray diffraction parameters and reaction rate modeling for gasification and combustion of chars derived from inertinite-rich coals. Fuel, 109(0): 148-156.

Faiz, M., Saghafi, A., Sherwood, N. and Wang, I., 2007. The influence of petrological properties and burial history on coal seam methane reservoir characterisation, Sydney Basin, Australia. International Journal of Coal Geology, 70(1-3): 193-208.

Faiz, M.M., Aziz, N.I., Hutton, A.C. and Jones, B.G., 1992. Porosity and gas sorption capacity of some eastern Australian coals in relation to coal rank and composition, Symp. Coalbed Methane Res. and Develop., Dept. of Earth Sci., James Cook Univ., Townsville, pp. 9–20.

Fu, Y., Liu, X., Ge, B. and Liu, Z., 2017. Role of chemical structures in coalbed methane adsorption for anthracites and bituminous coals. Adsorption, 23(5): 711-721.

Gasem, K.A.M., Robinson, J., L. and Reeves, S.R., 2002a. Adsorption of pure methane, nitroge and carbon dioxide and their mixtures on San Juan Basin coals. Topical Report.

Gasem, K.A.M., Sudibandriyo, M., Fitzgerald, J.E., Pan, Z. and Robinson Jr., R.L., 2002b. Measurement and modelling of gas adsorption on selected coals. Proceesings of the AICHE Spring National Meeting, New Orleans, Lousiana, March 10-16, 2002.

Gensterblum, Y., Busch, A. and Krooss, B.M., 2014a. Molecular concept and experimental evidence of competitive adsorption of H2O, CO2 and CH4 on organic material. Fuel, 115: 581-588.

Gensterblum, Y., Merkel, A., Busch, A. and Krooss, B.M., 2013. High-pressure CH4 and CO2 sorption isotherms as a function of coal maturity and the influence of moisture. International Journal of Coal Geology, 118(0): 45-57.

Gensterblum, Y., Merkel, A., Busch, A., Krooss, B.M. and Littke, R., 2014b. Gas saturation and CO2 enhancement potential of coalbed methane reservoirs as a function of depth. AAPG Bulletin, 98(2): 395-420.

Giffin, S., Littke, R., Klaver, J. and Urai, J.L., 2013. Application of BIB–SEM technology to characterize macropore morphology in coal. International Journal of Coal Geology, 114: 85-95.

Given, P.H., Marzec, A., Barton, W.A., Lynch, L.J. and Gerstein, B.C., 1986. The concept of a mobile or molecular phase within the macromolecular network of coals: A debate. Fuel, 65(2): 155-163.

Goñi, M.A. and Hedges, J.I., 1992. Lignin dimers: Structures, distribution, and potential geochemical applications. Geochimica et Cosmochimica Acta, 56(11): 4025-4043.

Gorbaty, M.L., Larsen, J.W. and Wende, I., 2013. Coal Science,. Academic Press.

Guo, X., Huan, X. and Huan, H., 2017. Structural Characteristics of Deformed Coals with Different Deformation Degrees and Their Effects on Gas Adsorption. Energy & fuels, 31(12): 13374-13381.

Gürdal, G. and Yalcin, M.N., 2001. Pore volume and surface area of the Carboniferous coals from the Zonguldak basin (NW Turkey) and their variations with rank and maceral composition. International Journal of Coal Geology, 48: 133-144.

Harpalani, S., Prusty, B.K. and Dutta, P., 2006. Methane/CO2 sorption modeling for coalbed methane production and CO2 sequestration. Energy and Fuels, 20: 1591-1599.

Hatcher, P.G. and Clifford, D.J., 1997. The organic geochemistry of coal: from plant materials to coal. Organic Geochemistry, 27(5): 251-274.

Hatcher, P.G. and Lerch, H.E., 1991. Survival of lignin-derived structural units in ancient coalified wood samples, Coal Science II. ACS Symposium Series. American Chemical Society, pp. 9-19.

Hatcher, P.G., Lerch, H.E. and Verheyen, T.V., 1990. Organic geochemical studies of the transformation of gymnospermous xylem during peatification and coalification to subbituminous coal. International Journal of Coal Geology, 16(1): 193-196.

Hattingh, B.B., Everson, R.C., Neomagus, H.W.J.P., Bunt, J.R., van Niekerk, D., Jordaan, J.H.L. and Mathews, J.P., 2013. Elucidation of the structural and molecular properties of typical South African coals. Energy & Fuels, 27(6): 3161-3172.

He, L., Cheng, G. and Melnichenko, Y.B., 2012a. Partial collapse and reswelling of a polymer in the critical demixing region of good solvents. Physical Review Letters, 109(6): 067801.

He, L., Melnichenko, Y.B., Mastalerz, M., Sakurovs, R., Radlinski, A.P. and Blach, T., 2012b. Pore accessibility by methane and carbon dioxide in coal as determined by neutron scattering. Energy & Fuels, 26(3): 1975-1983.

Hedges, J.I. and Mann, D.C., 1979. The characterization of plant tissues by their lignin oxidation products. Geochimica et Cosmochimica Acta, 43(11): 1803-1807.

Hildenbrand, A., Krooss, B.M., Busch, A. and Gaschnitz, R., 2006. Evolution of methane sorption capacity of coal seams as a function of burial history - A case study from the Campine Basin, NE Belgium. International Journal of Coal Geology, 66(3): 179-203.

Hirsch, P.B., 1954. X-Ray Scattering from Coals. Proceedings of the Royal Society of London. Series A. Mathematical and Physical Sciences, 226(1165): 143-169.

Hou, H., Shao, L., Li, Y., Li, Z., Wang, S., Zhang, W. and Wang, X., 2017. Influence of coal petrology on methane adsorption capacity of the Middle Jurassic coal in the Yuqia Coalfield, northern Qaidam Basin, China. Journal of Petroleum Science and Engineering, 149: 218-227.

Jacops, E., Aertsens, M., Maes, N., Bruggeman, C., Krooss, B.M., Amann-Hildenbrand, A., Swennen, R. and Littke, R., 2017. Interplay of molecular size and pore network geometry on the diffusion of dissolved gases and HTO in Boom Clay. Applied Geochemistry, 76: 182–195.

Jex, C.N., Pate, G.H., Blyth, A.J., Spencer, R.G.M., Hernes, P.J., Khan, S.J. and Baker, A., 2014. Lignin biogeochemistry: from modern processes to Quaternary archives. Quaternary Science Reviews, 87: 46-59.

Ji, L., Zhang, T., Milliken, K.L., Qu, J. and Zhang, X., 2012. Experimental investigation of main controls to methane adsorption in clay-rich rocks. Applied Geochemistry, 27(12): 2533-2545.

Jolliffe, I.T. and Cadima, J., 2016. Principal component analysis: a review and recent developments. Philosophical Transactions of the Royal Society A: Mathematical, Physical and Engineering Sciences, 374(2065): 20150202.

Joubert, J.I., Clifford, T. and Bienstock, D., 1973. Sorption of Methane in moist coal. Fuel, 52: 181-185.

Joubert, J.I., Grein, T. and Bienstock, D., 1974. Effect of moisture on the methane capacity of American coals. Fuel, 53: 186-191.

Karacan, C.Ö. and Olea, R.A., 2018. Mapping of compositional properties of coal using isometric log-ratio transformation and sequential Gaussian simulation – A comparative study for spatial ultimate analyses data. Journal of Geochemical Exploration, 186: 36-49.

Keiluweit, M., Nico, P.S., Johnson, M.G. and Kleber, M., 2010. Dynamic Molecular Structure of Plant Biomass-Derived Black Carbon (Biochar). Environmental Science & Technology, 44(4): 1247-1253.

Killingley, J.L., J. & Day, J., 1995. Methane adsorption on coals of the Bowen Basin, Queensland, Australia. Intergas, Univ. of Alabama, Tuscaloosa.

Krooss, B.M., van Bergen, F., Gensterblum, Y., Siemons, N., Pagnier, H.J.M. and David, P., 2002. High-pressure methane and carbon dioxide adsorption on dry and moisture-equilibrated Pennsylvanian coals. International Journal of Coal Geology, 51: 69-92.

Kurniawan, Y., Bhatia, S.K. and Rudolph, V., 2006. Simulation of binary mixture adsorption of methane and CO2 at supercritical conditions in carbons. AICHE Journal, 52: 957-967.

Lamberson, M.N. and Bustin, R.M., 1993. Coalbed methane characteristics of Gates formation coals, Northeastern British Columbia: Effect of maceral composition. AAPG Bulletin, 77(12): 2062-2076.

Laskar, D., Ke, D.D., Zeng, J., Gao, J. and Chen, X., 2012. Py-GC/MS as a powerful and rapid tool for determining lignin compositional and structural changes in biological processes, 9.

Laxminarayana, C. and Crosdale, P.J., 1999. Role of coal type and rank on methane sorption characteristics of Bowen Basin, Australia coals. international Journal of Coal Geology, 40: 309-325.

Laxminarayana, C. and Crosdale, P.J., 2002. Controls on methane sorption capacity of Indian coals. AAPG Bulletin, 86(2): 201-212.

Levy, J.H., Day, S.J. and Killingley, J.S., 1997. Methane capacities of Bowen Basin coals related to coal properties. Fuel, 76(9): 813-819.

Li, D., Liu, Q., Weniger, P., Gensterblum, Y., Busch, A. and Krooss, B.M., 2010. High-pressure sorption isotherms and sorption kinetics of CH4 and CO2 on coals. Fuel, 89(3): 569-580.

Li, K., Khanna, R., Zhang, J., Barati, M., Liu, Z., Xu, T., Yang, T. and Sahajwalla, V., 2015. Comprehensive investigation of various structural features of bituminous coals using advanced analytical techniques. Energy & Fuels, 29(11): 7178-7189.

Li, M., Zeng, F., Chang, H., Xu, B. and Wang, W., 2013. Aggregate structure evolution of low-rank coals during pyrolysis by in-situ X-ray diffraction. International Journal of Coal Geology(0): 262-269.

Liu, X. and He, X., 2017. Effect of pore characteristics on coalbed methane adsorption in middle-high rank coals. Adsorption, 23(1): 3-12.

Logan, K.J. and Thomas, B.A., 1985. Distribution of lignin derivatives in plants. The New Phytologist, 99(4): 571-585.
Logan, K.J. and Thomas, B.A., 1987. The distribution of lignin derivatives in fossil plants. The New Phytologist, 105(1): 157-173.
Lu, L., Sahajwalla, V., Kong, C. and Harris, D., 2001. Quantitative X-ray diffraction analysis and its application to various coals. Carbon, 39: 1821–1833.
MacKay, A.A. and Gschwend, P.M., 2000. Sorption of monoaromatic hydrocarbons to wood. Environmental Science & Technology, 34(5): 839-845.
Magill, C.R., Denis, E.H. and Freeman, K.H., 2015. Rapid sequential separation of sedimentary lipid biomarkers via selective accelerated solvent extraction. Organic Geochemistry, 88: 29-34.
Mahajan, O.P., 1982. Coal Porosity. In: R.A. Meyers (Editor), Coal Structure. Academic Press, pp. 51-86.
Mahajan, O.P., 1991. CO2 surface area of coals: The 25-year paradox. Carbon, 29(6): 735-742.
Maity, S. and Mukerjee, P., 2006. X-ray structural parameters of some Indian coals. Current Research, 91(3): 337-340.
Manoj, B., 2016. A comprehensive analysis of various structural parameters of Indian coals with the aid of advanced analytical tools. International Journal of Coal Science & Technology, 3(2): 123-132.
Manoj, B. and Kunjomana, A.G., 2012. Study of stacking structure of amorphous carbon by X-ray diffraction technique. International Journal of Electrochemical Science, 7(4): 3127-3134.
Marques, M., Suárez-Ruiz, I., Flores, D., Guedes, A. and Rodrigues, S., 2009. Correlation between optical, chemical and micro-structural parameters of high-rank coals and graphite. International Journal of Coal Geology, 77(3–4): 377-382.
Marsh, H., 1987. Adsorption methods to study microporosity in coals and carbons—a critique. Carbon, 25(1): 49-58.
Mathews, J.P. and Sharma, A., 2012. The structural alignment of coal and the analogous case of Argonne Upper Freeport coal. Fuel, 95: 19-24.
Milewska-Duda, J., Duda, J., Nodzenzski, A., Lakatos, J., 2000. Absorption and Adsorption of Methane and Carbon Dioxide in Hard Coal and Active Carbon. Langmuir, 16: 5458-5466.
Millward, G.R., 1979. Coal and Modern Coal Processing: An Introduction. Academic Press: New York.
Nandi, S.P. and Walker Jr., P.L., 1970. Activated diffusion of methane in coal. Fuel, 49: 309-323.
Narkiewicz, M.R. and Mathews, J.P., 2008. Improved low-volatile bituminous coal representation: Incorporating the molecular-weight distribution. Energy & Fuels, 22(5): 3104-3111.
Nelson, E.T. and Walker, P.L., 1961. Some techniques for investigating the unsteady-state molecular flow of gas through a microporous medium. Journal of Applied Chemistry, 11(9): 358-364.
Nelson, J.B., 1954. X-Ray Studies of the ultra-fine structure of coal I-Low-angle scattering of vitrinite from coals of differing rank Fuel, 22: 153-175.
Nie, B., Liu, X., Yuan, S., Ge, B., Jia, W., Wang, C. and Chen, X., 2016. Sorption charateristics of methane among various rank coals: impact of moisture. Adsorption: 1-11.
Nishino, J., 2001. Adsorption of water vapor and carbon dioxide at carboxylic functional groups on the surface of coal. Fuel, 80: 757-764.
Novo-Uzal, E., Pomar, F., Gómez Ros, L.V., Espiñeira, J.M. and Ros Barceló, A., 2012. Evolutionary history of lignins. In: L. Jouanin and C. Lapierre (Editors), Advances in Botanical Research. Academic Press, pp. 309-350.
Oberlin, A., Villey, M. and Combaz, A., 1980. Influence of elemental composition on carbonization: Pyrolysis of kerosene shale and kuckersite. Carbon, 18(5): 347-353.
Okolo, G.N., Neomagus, H.W.J.P., Everson, R.C., Roberts, M.J., Bunt, J.R., Sakurovs, R. and Mathews, J.P., 2015. Chemical–structural properties of South African bituminous coals: Insights from wide angle XRD–carbon fraction analysis, ATR–FTIR, solid state 13C NMR, and HRTEM techniques. Fuel, 158: 779-792.
Pan, J., Hou, Q., Ju, Y., Bai, H. and Zhao, Y., 2012. Coalbed methane sorption related to coal deformation structures at different temperatures and pressures. Fuel, 102(0): 760-765.
Papa, G., Scaglia, B., Schievano, A. and Adani, F., 2014. Nanoscale structure of organic matter could explain litter decomposition. Biogeochemistry, 117(2-3): 313-324.
Pashin, J.C., Carroll, R.E., Groshong Jr., R.H., Raymond, D.E., McIntyre, M.R. and Payton, J.W., 2004. Geologic screening criteria for sequestration of CO2 in coal: quantifying potential of the Black Warrior coalbed methane fairway. , Alabama. U.S. Dept. of Energy, Final Tech. Rept., DE-FC26-00NT40927.

Peters, K.E., Walters, C.C. and Moldowan, J.M., 2005. The Biomarker Guide: Biomarkers and Isotopes in Petroleum Exploration and Earth History. Cambridge University Press, United Kingdom.

Pini, R., Ottiger, S., Burlini, L., Storti, G., Mazzotti, M., Bencini, R. and Quattrocchi, F., 2006. Experimental study of CO2 sequestration by ECBM recovery: the case of Sulcis coal, GHGT8, Trondheim, Norway.

Pittermann, J., 2010. The evolution of water transport in plants: an integrated approach. Geobiology, 8(2): 112-39.

Prinz, D. and Littke, R., 2005. Development of the micro- and ultramicroporous structure of coals with rank as deduced from the accessibility to water. Fuel, 84(12-13): 1655-1662.

Prinz, D., Pyckhout-Hintzen, W. and Littke, R., 2004. Development of the meso- and macroporous structure of coals with rank as analyzed with small angle neutron scattering and adsorption experiments. Fuel, 83: 547-556.

Radovic, L.R., Menon, V.C., Leon Y Leon, C.A., Kyotani, T., Danner, R.P., Anderson, S. and Hatcher, P.G., 1997. On the porous structure of coals: Evidence for an interconnected but constricted micropore system and implications for coalbed methane recovery. Adsorption, 3(3): 221-232.

Radovic, L.R., Menon, V.C., Leon Y Leon, C.A., Kyotani, T., Danner, R.E., Anderson, S., Hatcher, P.G., 1997. On the Porous Structure of Coals: Evidence for an Interconnected but Constricted Micropore System and Implications for Coalbed Methane Recovery*. Adsorption, 3: 221-232.

Ran, Y., Yang, Y., Xing, B., Pignatello, J.J., Kwon, S., Su, W. and Zhou, L., 2013. Evidence of micropore filling for sorption of nonpolar organic contaminants by condensed organic matter. J Environ Qual, 42(3): 806-14.

Reeves, S., Gonzalez, R., Gasem, K.A.M., Fitzgerald, J.E., Pan, Z., Sudibandriyo, M. and Robinson Jr., R.L., 2005. Measurement and prediction of single- and multi-component methane, carbon dioxide and nitrogen isotherms for U.S. coals, ICBM Symposium Tuscaloosa, Tuscaloosa, Alabama.

Rice, D.D., 1993. Composition and origins of coalbed gas. In: B.E. Law and D.D. Rice (Editors), Hydrocarbons from coal. AAPG studies in Geology, pp. 159-184.

Roberts, M.J., Everson, R.C., Neomagus, H.W.J.P., Okolo, G.N., Van Niekerk, D. and Mathews, J.P., 2015a. The characterisation of slow-heated inertinite- and vitrinite-rich coals from the South African coalfields. Fuel, 158: 591-601.

Roberts, M.J., Everson, R.C., Neomagus, H.W.J.P., Van Niekerk, D., Mathews, J.P. and Branken, D.J., 2015b. Influence of maceral composition on the structure, properties and behaviour of chars derived from South African coals. Fuel, 142(0): 9-20.

Rodrigues, S., Suárez-Ruiz, I., Marques, M., Camean, I. and Flores, D., 2011. Microstructural evolution of high temperature treated anthracites of different rank. International Journal of Coal Geology, 87(3–4): 204-211.

Rouzaud, J.N. and Oberlin, A., 1990. The characterisation of coals and cokes by electron transmission microscopy. In: H. Charcosset and B. Nickel-Pepin-Donat (Editors), Advanced Methodologies in Coal Characterization. Elsevier, pp. 311-355.

Ryan, B. and Lane, B., 2002. Adsorption characteristics of coal with special reference to the Gething Formation, Northeastern British Columbia, British Columbia Geological Survey (https://pdfs.semanticscholar.org/209b/5304438f9754c924b9dd853868d7e320f283.pdf?_ga=2.154767803.2077293256.1558123861-1808539235.1558123861).

Saghafi, A., 2010. Potential for ECBM and CO2 storage in mixed gas Australian coals. International Journal of Coal Geology, 82(3): 240-251.

Saikia, B., Boruah, R. and Gogoi, P., 2009. A X-ray diffraction analysis on graphene layers of Assam coal. Journal of Chemical Sciences, 121(1): 103-106.

Sarkar, P., Bosneaga, E. and Auer, M., 2009. Plant cell walls throughout evolution: towards a molecular understanding of their design principles. Journal of experimental botany, 60(13): 3615-3635.

Scott, A.C., 2002. Coal petrology and the origin of coal macerals: a way ahead? International Journal of Coal Geology, 50(1-4): 119-134.

Shan, C., Zhang, T., Liang, X., Zhang, Z., Zhu, H., Yang, W. and Zhang, K., 2018. Influence of chemical properties on CH4 adsorption capacity of anthracite derived from southern Sichuan Basin, China. Marine and Petroleum Geology, 89: 387-401.

Sharma, A., Kyotani, T. and Tomita, A., 2000. Direct Observation of Raw Coals in Lattice Fringe Mode Using High-Resolution Transmission Electron Microscopy. Energy & Fuels, 14(6): 1219-1225.

Shinn, J.H., 1984. From coal to single-stage and two-stage products: A reactive model of coal structure. Fuel, 63(9): 1187-1196.
Smoot, L.D. and Smith, P.J., 2013. Coal Combustion and Gasification. Springer Science & Business Media: New York.
Sonibare, O.O., Haeger, T. and Foley, S.F., 2010. Structural characterization of Nigerian coals by X-ray diffraction, Raman and FTIR spectroscopy. Energy, 35(12): 5347-5353.
Sperry, John S., 2003. Evolution of Water Transport and Xylem Structure. International Journal of Plant Sciences, 164(S3): S115-S127.
Spiro, C.L., 1981. Space-filling models for coal: a molecular description of coal plasticity. Fuel, 60(12): 1121-1126.
Tang, J. and Weber, W.J., Jr., 2006. Development of engineered natural organic sorbents for environmental applications. 2. Sorption characteristics and capacities with respect to phenanthrene. Environ Sci Technol, 40(5): 1657-63.
Tao, S., Chen, S., Tang, D., Zhao, X., Xu, H. and Li, S., 2018. Material composition, pore structure and adsorption capacity of low-rank coals around the first coalification jump: A case of eastern Junggar Basin, China. Fuel, 211: 804-815.
Taylor, G.H., Teichmüller, M., Davis, A., Diessel, C.F.K., Littke, R. and Robert, P., 1998. Organic Petrology. Gebr. Borntraeger, Berlin-Stuttgart, 704 pp.
Tsiao, C. and Botto, R.E., 1991. Xenon-129 NMR investigation of coal micropores. Energy & Fuels, 5(1): 87-92.
van Krevelen, D.W., 1993. Coal: Typology-Physics-Chemistry-Constitution. Elsevier, 1002 pp.
Van Niekerk, D., Pugmire, R.J., Solum, M.S., Painter, P.C. and Mathews, J.P., 2008. Structural characterization of vitrinite-rich and inertinite-rich Permian-aged South African bituminous coals. International Journal of Coal Geology, 76(4): 290-300.
Walker, P.L. and Mahajan, O.P., 1993. Pore structure in coals. Energy & Fuels, 7(4): 559-560.
Walker, P.L., Spinks, A., Thomas, J.M. and Gibson, J., 1981. Microporosity in coal: its characterization and its implications for coal utilization. Philosophical Transactions of the Royal Society of London. Series A, Mathematical and Physical Sciences, 300(1453): 65-81.
Wang, L., Chen, E.-T., Liu, S., Cheng, Y.-P., Cheng, L.-B., Chen, M.-Y. and Guo, H.-J., 2017. Experimental study on the effect of inherent moisture on hard coal adsorption–desorption characteristics. Adsorption, 23(5): 723-742.
Wang, X., Cook, R., Tao, S. and Xing, B., 2007. Sorption of organic contaminants by biopolymers: Role of polarity, structure and domain spatial arrangement. Chemosphere, 66(8): 1476-1484.
Weng, J.K., Li, X., Stout, J. and Chapple, C., 2008. Independent origins of syringyl lignin in vascular plants. Proc Natl Acad Sci U S A, 105(22): 7887-92.
Weniger, P., Francu, J., Hemza, P. and Krooss, B.M., 2012. Investigations on the methane and carbon dioxide sorption capacity of coals from the SW Upper Silesian Coal Basin, Czech Republic. International Journal of Coal Geology, 93: 23–39.
Weniger, P., Kalkreuth, W., Busch, A. and Krooss, B.M., 2010. High-pressure methane and carbon dioxide sorption on coal and shale samples from the Paraná Basin, Brazil. International Journal of Coal Geology, 84(3-4): 190-205.
Wertz, D.L. and Bissell, M., 1994. Relating the nonideal diffraction from the graphene layer stacking peak to the aliphatic carbon abundance in bituminous coals. Energy & Fuels, 8(3): 613-617.
Yao, Y., Liu, D., Tang, D., Tang, S., Che, Y. and Huang, W., 2009. Preliminary evaluation of the coalbed methane production potential and its geological controls in the Weibei Coalfield, Southeastern Ordos Basin, China. International Journal of Coal Geology, 78(1): 1-15.
Yao, Y., Liu, D., Tang, D., Tang, S. and Huang, W., 2008. Fractal characterization of adsorption-pores of coals from North China: An investigation on CH4 adsorption capacity of coals. International Journal of Coal Geology, 73(1): 27-42.
Zhang, L. and LeBoeuf, E.J., 2009. A molecular dynamics study of natural organic matter: 1. Lignin, kerogen and soot. Organic Geochemistry, 40(11): 1132-1142.
Zhang, T., Ellis, G.S., Ruppel, S.C., Milliken, K. and Yang, R., 2012. Effect of organic-matter type and thermal maturity on methane adsorption in shale-gas systems. Organic Geochemistry, 47: 120-131.

Zhao, J., Xu, H., Tang, D., Mathews, J.P., Li, S. and Tao, S., 2016. A comparative evaluation of coal specific surface area by CO2 and N2 adsorption and its influence on CH4 adsorption capacity at different pore sizes. Fuel, 183: 420-431.

Zhao, L., Qin, Y., Cai, C., Xie, Y., Wang, G., Huang, B. and Xu, C., 2017. Control of coal facies to adsorption-desorption divergence of coals: A case from the Xiqu Drainage Area, Gujiao CBM Block, North China. International Journal of Coal Geology, 171: 169-184.

Zheng, G., Pan, Z., Chen, Z., Tang, S., Connell, L.D., Zhang, S. and Wang, B., 2012. Laboratory study of gas permeability and cleat compressibility for CBM/ECBM in Chinese coals. Energy Exploration and Exploitation, 30(3): 451–476.

Highlights

We present relationships between methane gas sorption capacity of coals and geochemical and petrophysical properties based on an extensive database.

Data shows evidence that the main determining factor for methane sorption capacity is paleoflora and therefore the differences between the Permian and the Carboniferous.

We find that the macromolecular structure and chemical properties (i.e., polarity or hydrophobicity) of lignin are likely to influence methane sorption in coals.

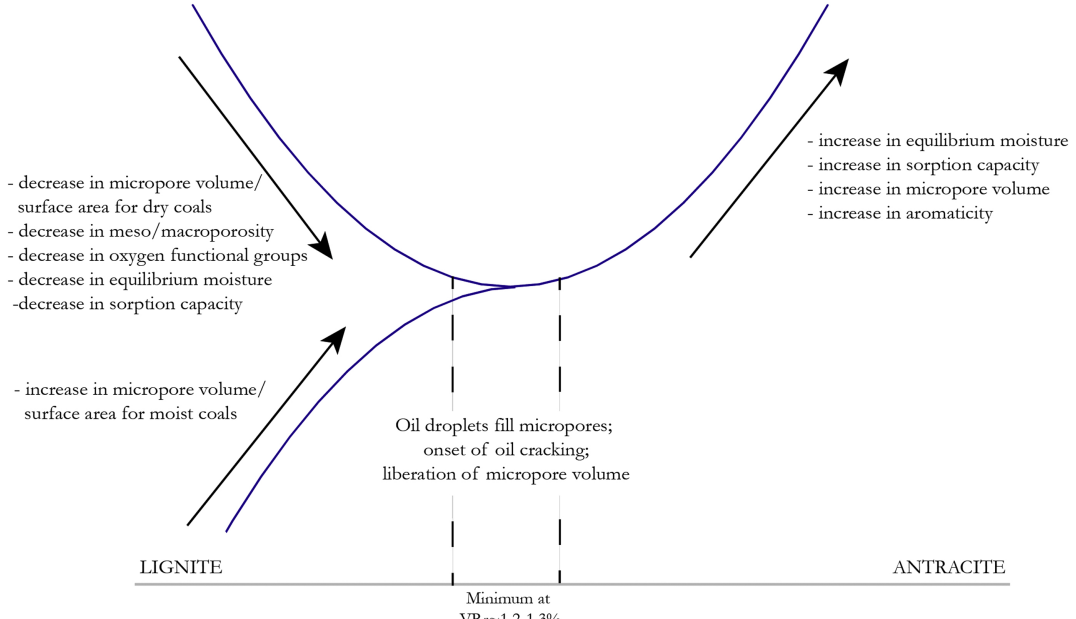
- decrease in micropore volume/
surface area for dry coals
- decrease in meso/macroporosity
- decrease in oxygen functional groups
- decrease in equilibrium moisture
-decrease in sorption capacity
- increase in micropore volume/
surface area for moist coals
- increase in equilibrium moisture
- increase in sorption capacity
- increase in micropore volume
- increase in aromaticity
Oil droplets fill micropores;
onset of oil cracking;
liberation of micropore volume
LIGNITE
ANTRACITE
Minimum at
VRr~1.2-1.3%

Figure 1

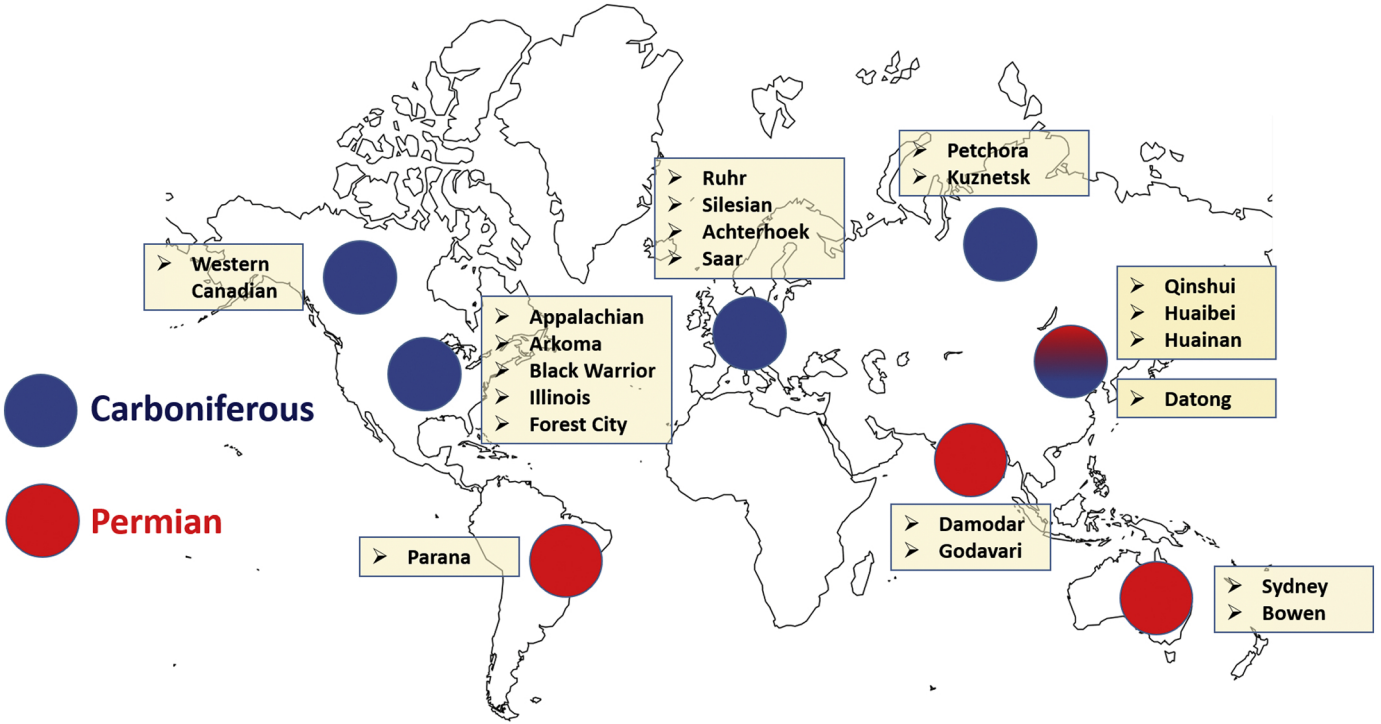
Carboniferous
Permian
Western Canadian
Appalachian
Arkoma
Black Warrior
Illinois
Forest City
Parana
Ruhr
Silesian
Achterhoek
Saar
Petchora
Kuznetsk
Qinshui
Huaibei
Huainan
Datong
Damodar
Godavari
Sydney
Bowen

Figure 2

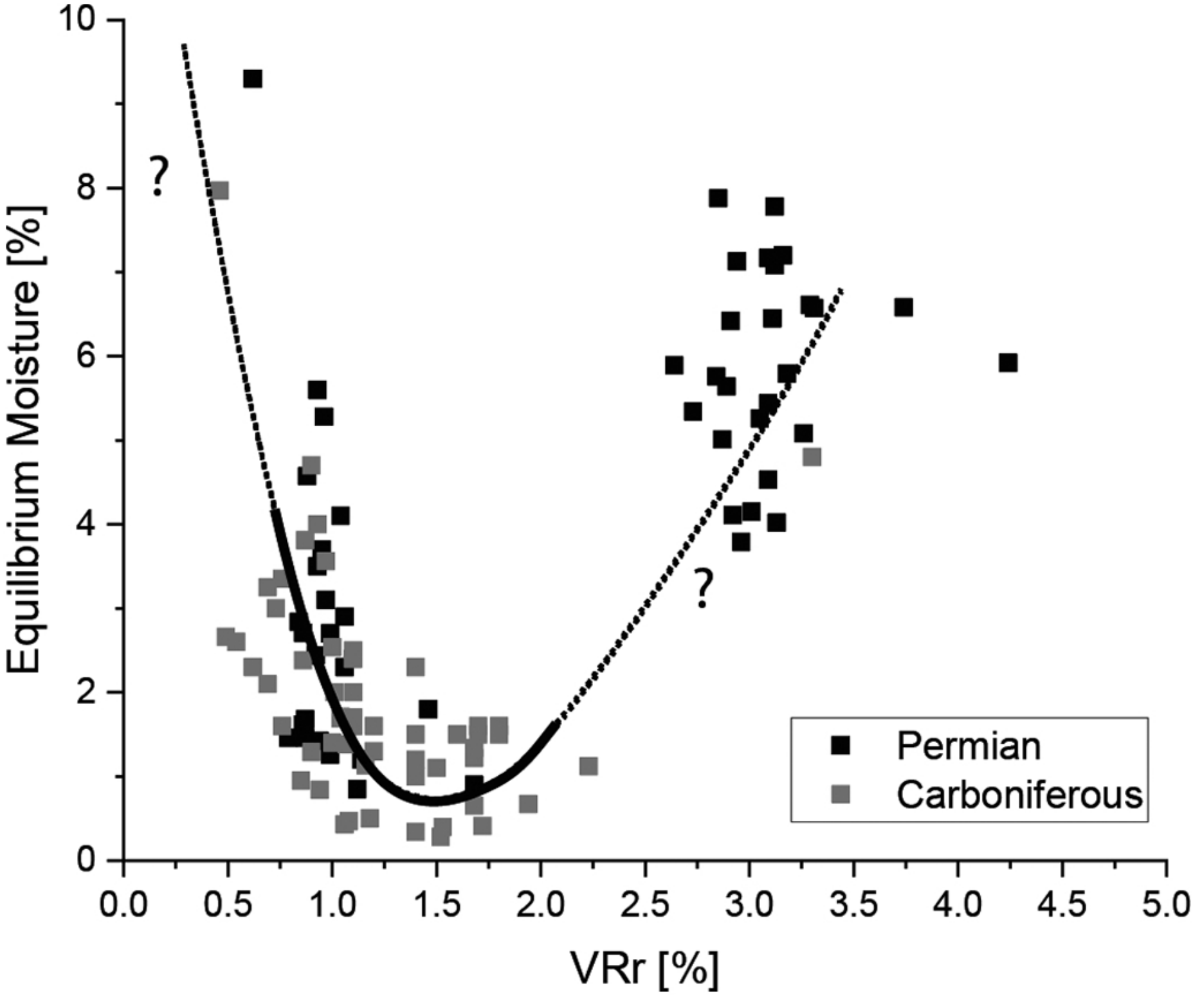
Equilibrium Moisture [%]
VRr [%]
Permian
Carboniferous
?
?
0
2
4
6
8
10
0.0
0.5
1.0
1.5
2.0
2.5
3.0
3.5
4.0
4.5
5.0

Figure 3

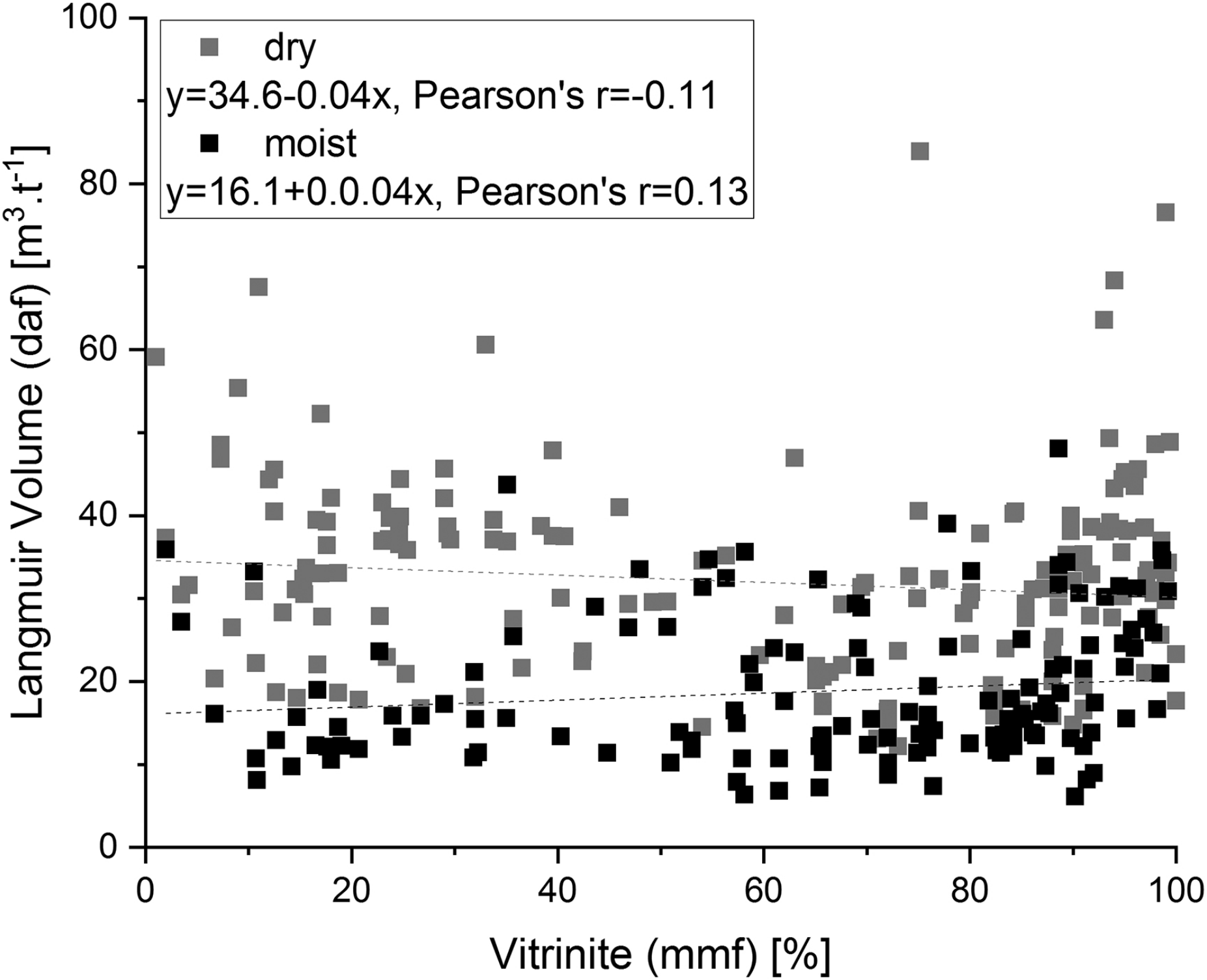
dry
y=34.6-0.04x, Pearson's r=-0.11
moist
y=16.1+0.0.04x, Pearson's r=0.13
Langmuir Volume (daf) [m3.t-1]
Vitrinite (mmf) [%]
0
20
40
60
80
100

Figure 4

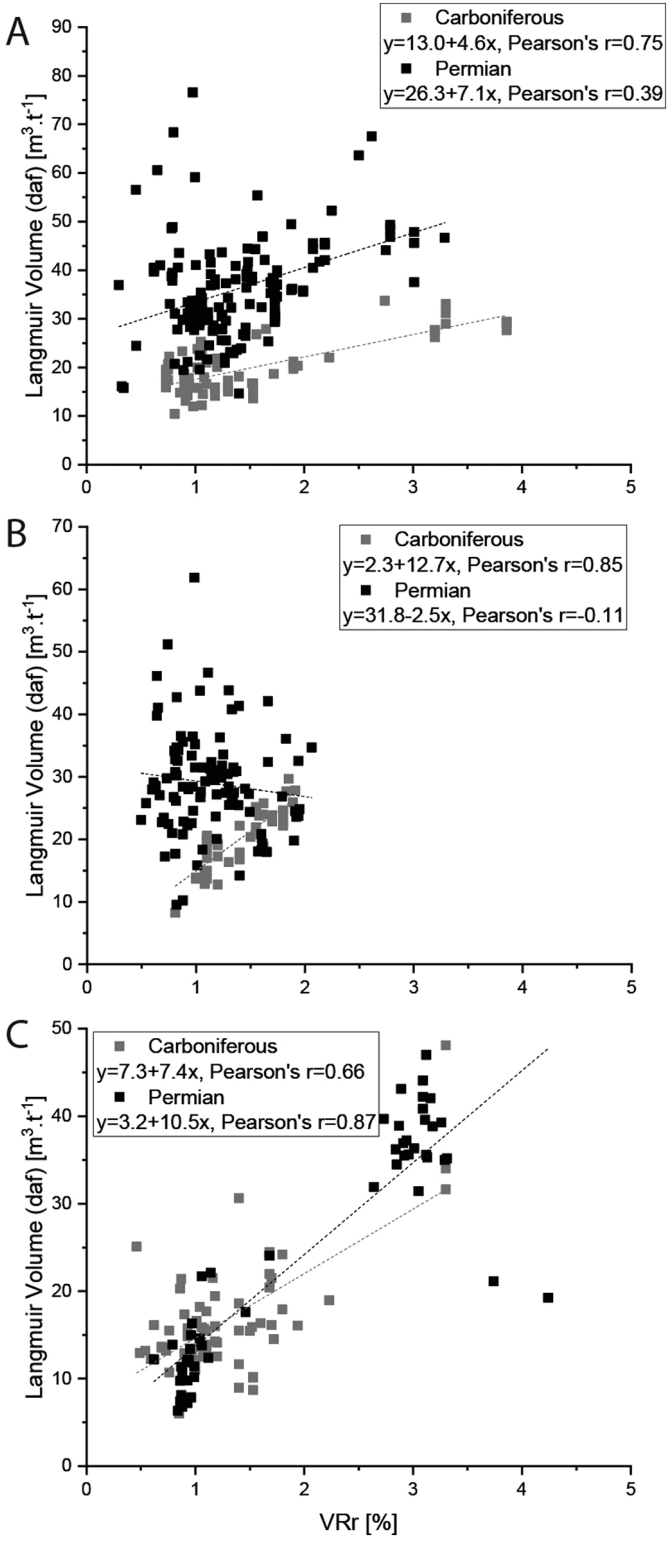
A
Carboniferous
y=13.0+4.6x, Pearson's r=0.75
Permian
y=26.3+7.1x, Pearson's r=0.39
Langmuir Volume (daf) [m3.t-1]
B
Carboniferous
y=2.3+12.7x, Pearson's r=0.85
Permian
y=31.8-2.5x, Pearson's r=-0.11
Langmuir Volume (daf) [m3.t-1]
C
Carboniferous
y=7.3+7.4x, Pearson's r=0.66
Permian
y=3.2+10.5x, Pearson's r=0.87
Langmuir Volume (daf) [m3.t-1]
VRr [%]

Figure 5

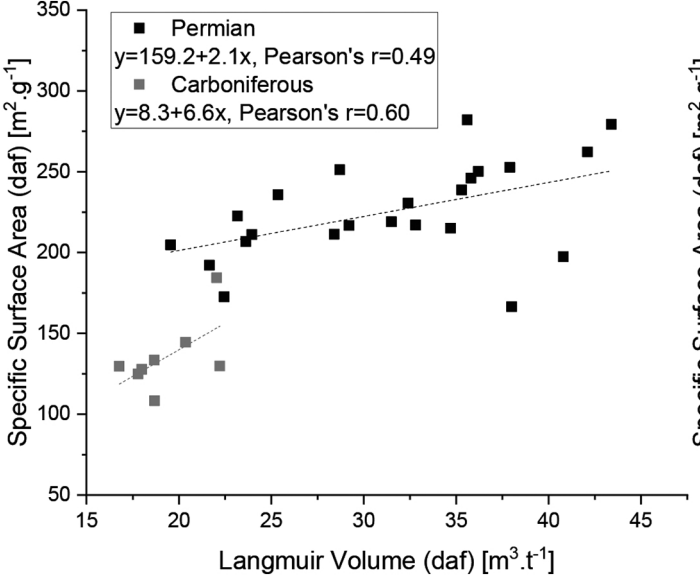
Permian
y=159.2+2.1x, Pearson's r=0.49
Carboniferous
y=8.3+6.6x, Pearson's r=0.60
Specific Surface Area (daf) [m2.g-1]
Langmuir Volume (daf) [m3.t-1]
350
300
250
200
150
100
50
15
20
25
30
35
40
45

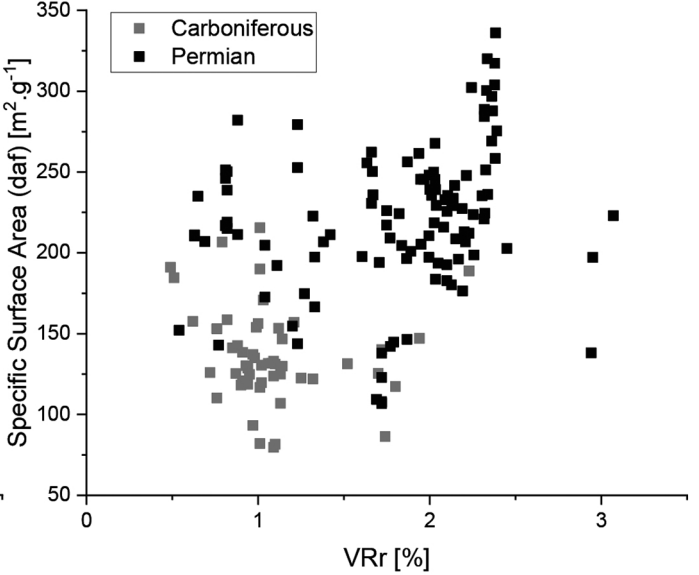
Carboniferous
Permian
Specific Surface Area (daf) [m2.g-1]
VRr [%]
350
300
250
200
150
100
50
0
1
2
3

Figure 6

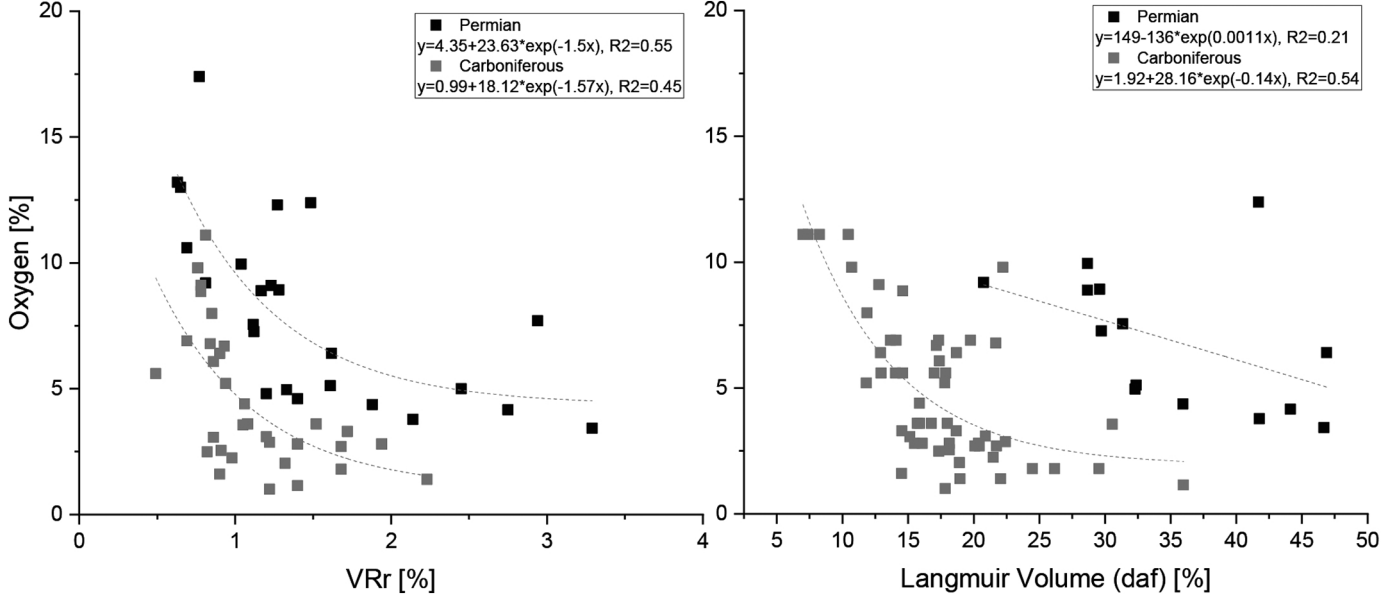
Permian
y=4.35+23.63*exp(-1.5x), R2=0.55
Carboniferous
y=0.99+18.12*exp(-1.57x), R2=0.45
Oxygen [%]
VRr [%]
Permian
y=149-136*exp(0.0011x), R2=0.21
Carboniferous
y=1.92+28.16*exp(-0.14x), R2=0.54
Langmuir Volume (daf) [%]

Figure 7

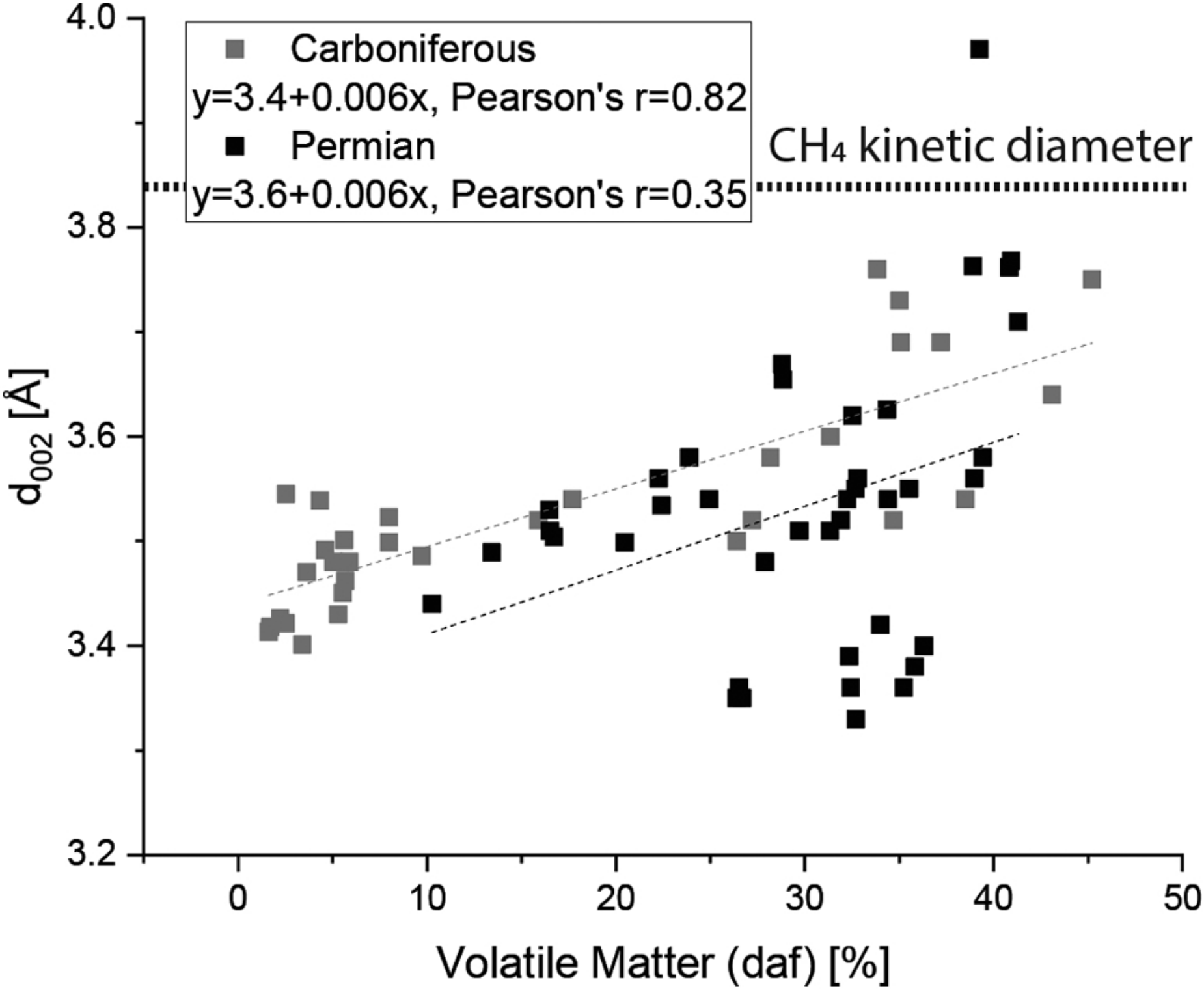
Carboniferous
y=3.4+0.006x, Pearson's r=0.82
Permian
y=3.6+0.006x, Pearson's r=0.35
CH4 kinetic diameter
d002 [Å]
4.0
3.8
3.6
3.4
3.2
0
10
20
30
40
50
Volatile Matter (daf) [%]

Figure 8

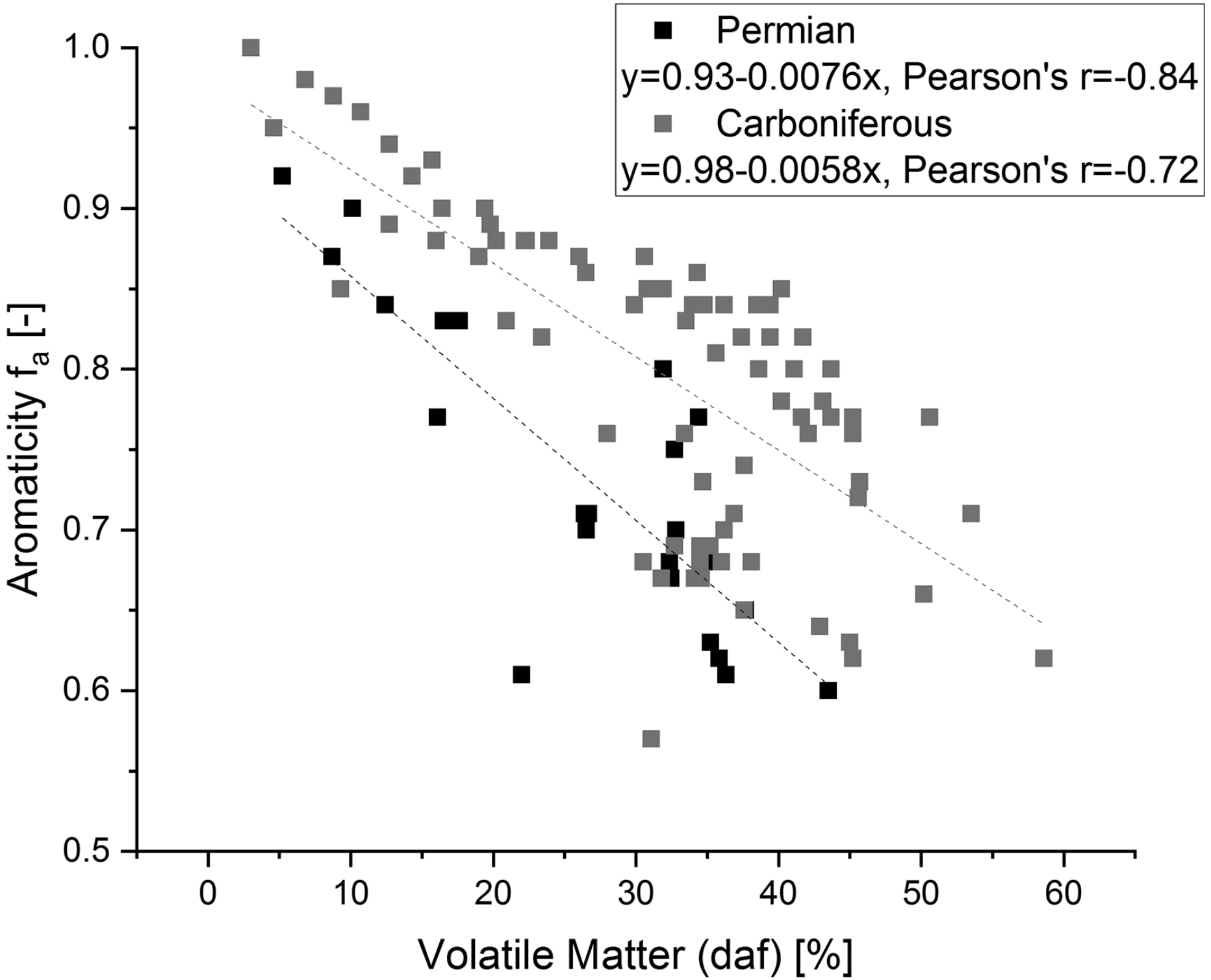
Permian
y=0.93-0.0076x, Pearson's r=-0.84
Carboniferous
y=0.98-0.0058x, Pearson's r=-0.72
Aromaticity f_a [-]
Volatile Matter (daf) [%]
1.0
0.9
0.8
0.7
0.6
0.5
0
10
20
30
40
50
60

Figure 9

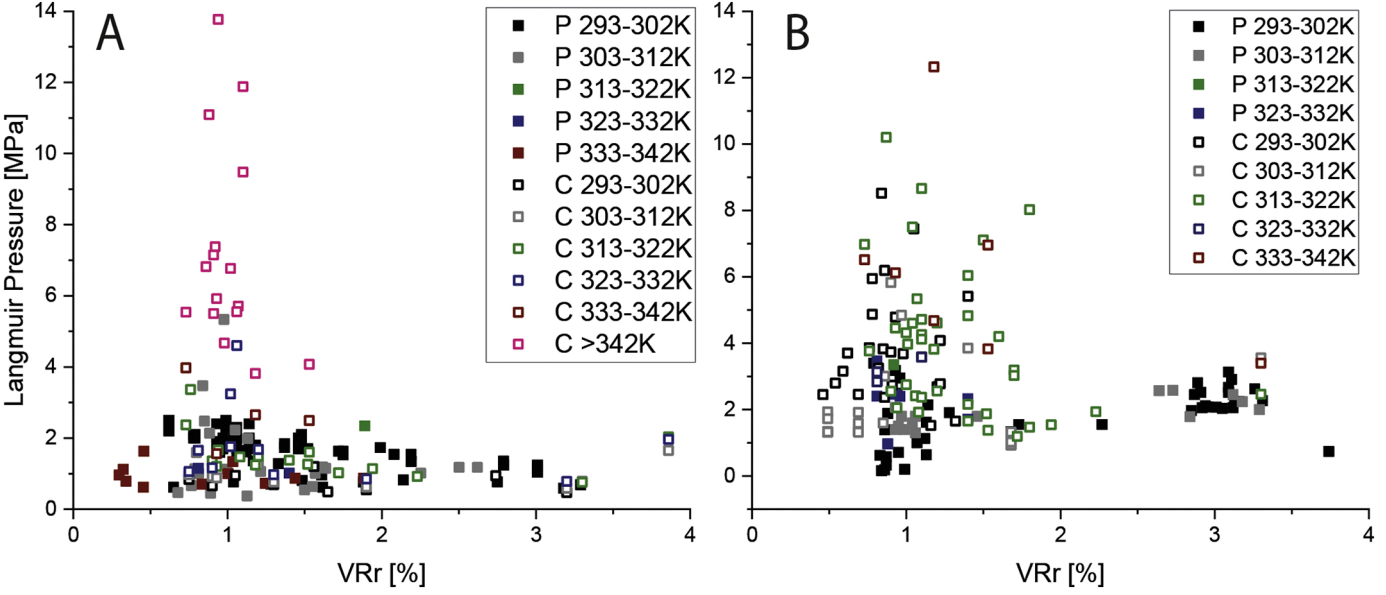
A
B
Langmuir Pressure [MPa]
VRr [%]
VRr [%]
P 293-302K
P 303-312K
P 313-322K
P 323-332K
P 333-342K
C 293-302K
C 303-312K
C 313-322K
C 323-332K
C 333-342K
C >342K
P 293-302K
P 303-312K
P 313-322K
P 323-332K
C 293-302K
C 303-312K
C 313-322K
C 323-332K
C 333-342K

Figure 10

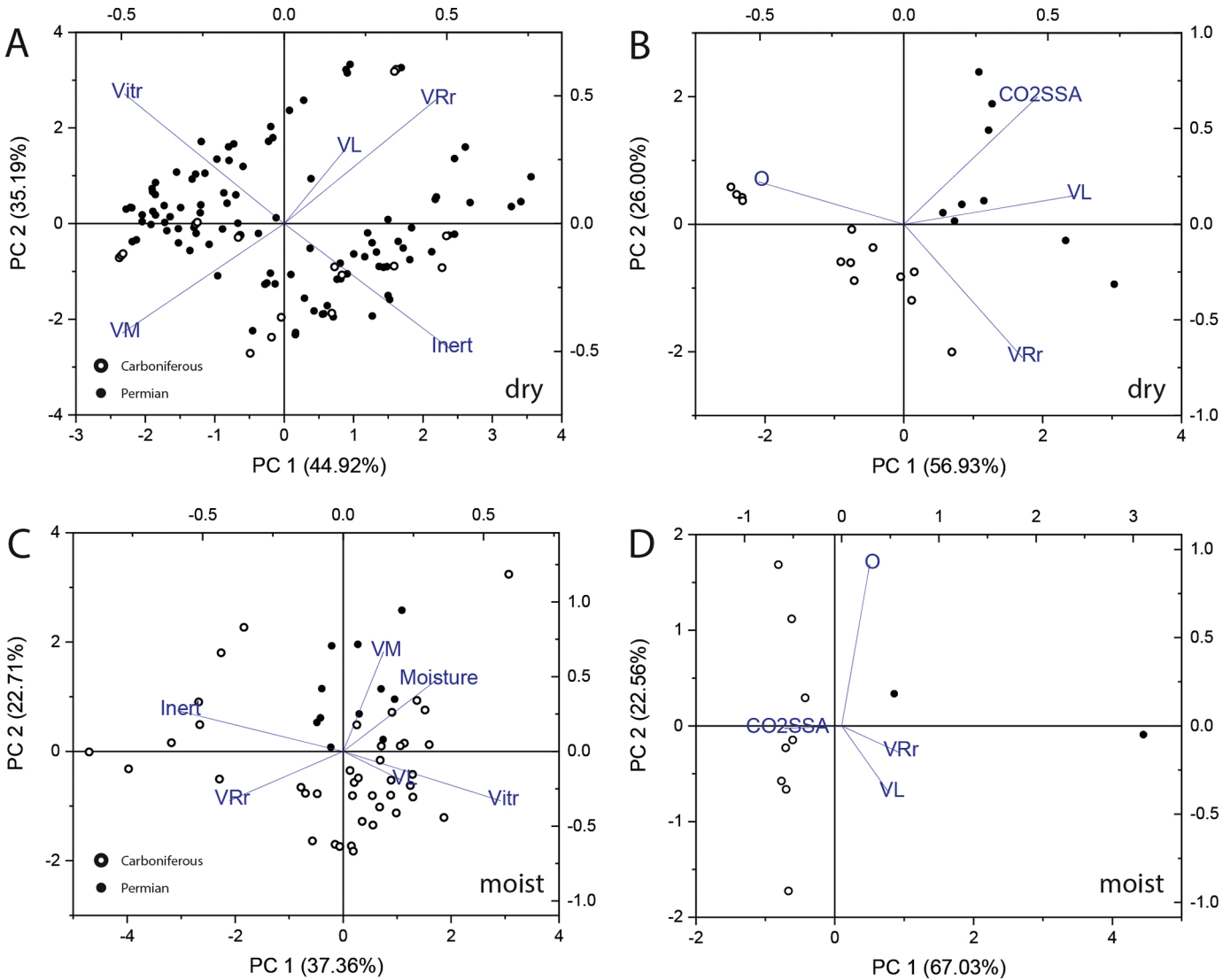
A
Vitr
VRr
VL
VM
Inert
Carboniferous
Permian
dry
PC 1 (44.92%)
PC 2 (35.19%)
B
CO2SSA
O
VL
VRr
dry
PC 1 (56.93%)
PC 2 (26.00%)
C
VM
Moisture
Inert
VRr
VL
Vitr
Carboniferous
Permian
moist
PC 1 (37.36%)
PC 2 (22.71%)
D
O
CO2SSA
VRr
VL
moist
PC 1 (67.03%)
PC 2 (22.56%)

Figure 11

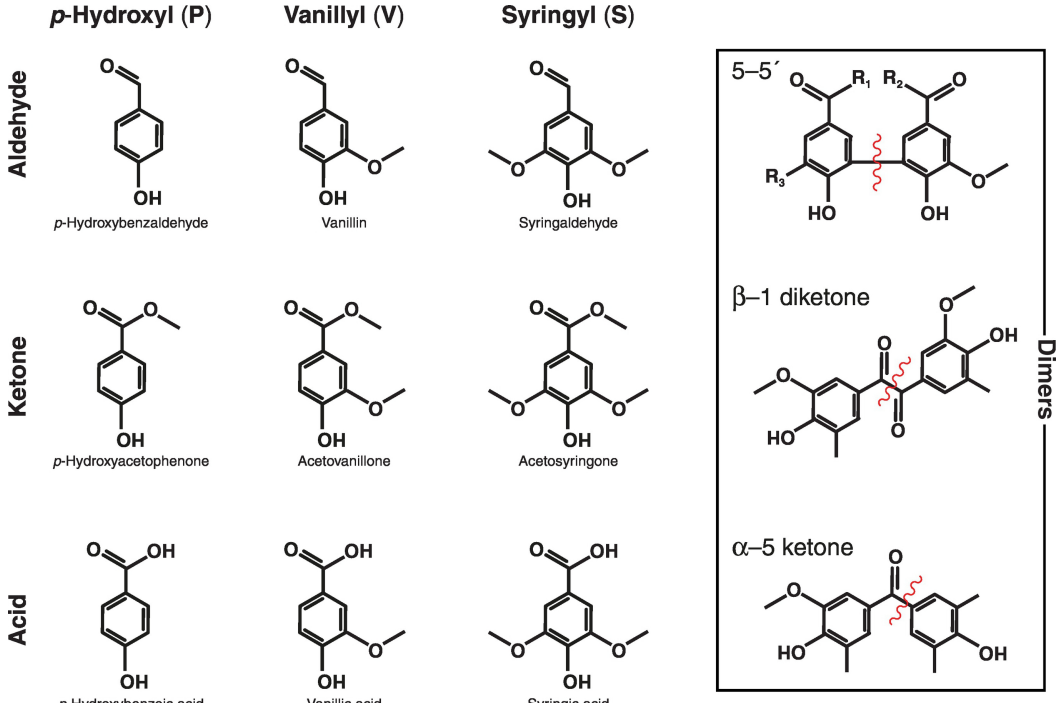
p-Hydroxyl (P)
Vanillyl (V)
Syringyl (S)
Aldehyde
Ketone
Acid
p-Hydroxybenzaldehyde
Vanillin
Syringaldehyde
p-Hydroxyacetophenone
Acetovanillone
Acetosyringone
p-Hydroxybenzoic acid
Vanillic acid
Syringic acid
5–5´
β–1 diketone
α–5 ketone
Dimers

Figure 12

Lipid biomarker	Common name	Source(s)
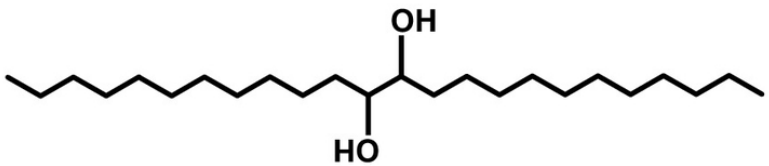	ω20-Dialcohol	Ferns
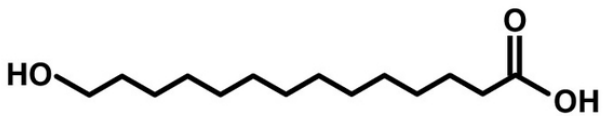	ω-C_{16} Hydroxyacids	Lycopods
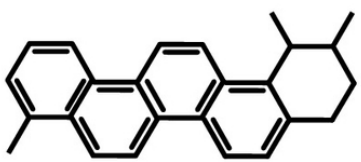	Triterpenoids	Angiosperms
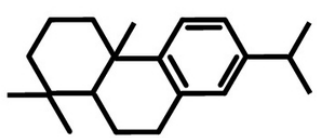	Diterpenoids	Gymnosperms
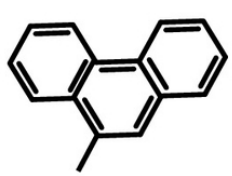	Methylphenanthrenes	Petroleum#

Figure 13

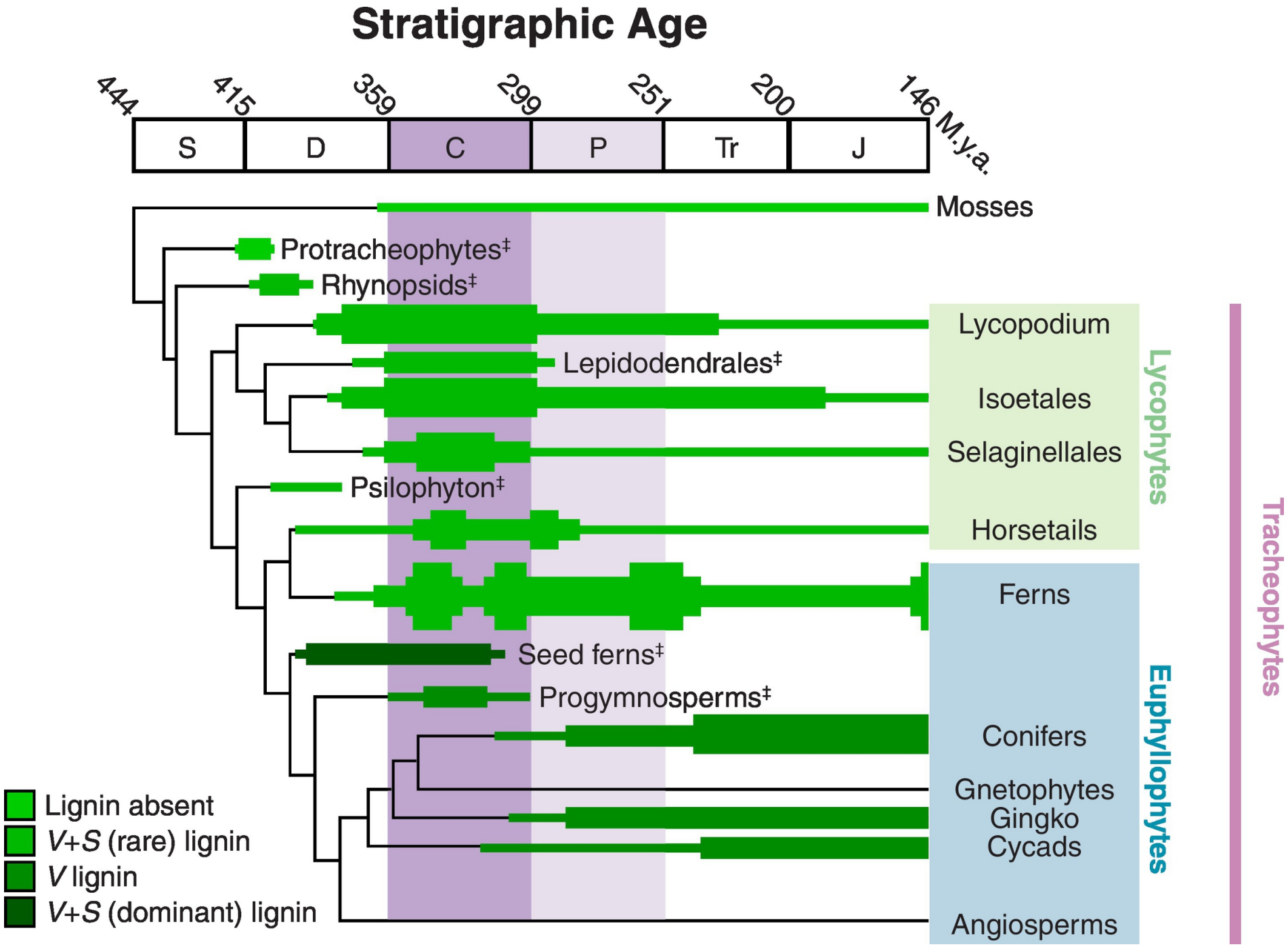
Stratigraphic Age
444
415
359
299
251
200
146 M.y.a.
S
D
C
P
Tr
J
Mosses
Protracheophytes‡
Rhynopsids‡
Lycopodium
Lepidodendrales‡
Isoetales
Selaginellales
Psilophyton‡
Horsetails
Ferns
Seed ferns‡
Progymnosperms‡
Conifers
Gnetophytes
Gingko
Cycads
Angiosperms
Lycophytes
Euphyllophytes
Tracheophytes
Lignin absent
V+S (rare) lignin
V lignin
V+S (dominant) lignin

Figure 14